Journal of Visualized Experiments

Dynamic Inter-Subject Functional Connectivity Reveals Moment-to-Moment Brain Network Configurations Driven by Continuous or Communication Paradigms

--Manuscript Draft--

Article Type:	Invited Methods Article - JoVE Produced Video
Manuscript Number:	JoVE59083R1
Full Title:	Dynamic Inter-Subject Functional Connectivity Reveals Moment-to-Moment Brain Network Configurations Driven by Continuous or Communication Paradigms
Keywords:	Functional magnetic resonance imaging Task-based analysis Dynamic functional connectivity Inter-subject functional correlation Sliding-window analysis Thresholding Movie-watching paradigm
Corresponding Author:	Thomas Bolton Ecole Polytechnique Federale de Lausanne Geneva, Geneva SWITZERLAND
Corresponding Author's Institution:	Ecole Polytechnique Federale de Lausanne
Corresponding Author E-Mail:	thomas.bolton@epfl.ch
Order of Authors:	Thomas Bolton
	Delphine Jochaut
	Anne-Lise Giraud
	Dimitri Van De Ville
Additional Information:	
Question	**Response**
Please indicate whether this article will be Standard Access or Open Access.	Open Access (US$4,200)
Please indicate the **city, state/province, and country** where this article will be **filmed**. Please do not use abbreviations.	Geneva, Geneva, Switzerland

TITLE:

Dynamic Inter-Subject Functional Connectivity Reveals Moment-to-Moment Brain Network Configurations Driven by Continuous or Communication Paradigms

AUTHORS AND AFFILIATIONS:

Thomas A.W. Bolton[1,2], Delphine Jochaut[3], Anne-Lise Giraud[3], Dimitri Van De Ville[1,2]

[1] Institute of Bioengineering, École Polytechnique Fédérale de Lausanne (EPFL), Lausanne, Switzerland
[2] Department of Radiology and Medical Informatics, University of Geneva, Geneva, Switzerland
[3] Department of Neuroscience, University of Geneva, Switzerland

Corresponding Author:
Thomas A.W. Bolton
thomas.bolton@epfl.ch

Email Addresses of Co-Authors:
Delphine Jochaut: delphine.jochaut@unige.ch
Anne-Lise Giraud: anne-lise.giraud@unige.ch
Dimitri Van De Ville: dimitri.vandeville@epfl.ch

KEYWORDS:

Functional magnetic resonance imaging, task-based analysis, dynamic functional connectivity, inter-subject functional correlation, sliding-window analysis, thresholding, movie-watching paradigm

SUMMARY:

The goal of the described approach is to determine at what moments of the paradigm (temporal perspective), and between which regions (spatial perspective), significant reconfigurations in functional connectivity occur on functional magnetic resonance imaging recordings during which a time-locked stimulus is played.

ABSTRACT:

Task-based functional magnetic resonance imaging bears great potential to understand how our brain reacts to various types of stimulation; however, this is often achieved without considering the dynamic facet of functional processing, and analytical outputs typically account for merged influences of task-driven effects and underlying spontaneous fluctuations of brain activity. Here, we introduce a novel methodological pipeline that can go beyond these limitations: the use of a sliding-window analytical scheme permits tracking of functional changes over time, and through cross-subject correlational measurements, the approach can isolate purely stimulus-related effects. Thanks to a rigorous thresholding process, significant changes in inter-subject functional correlation can be extracted and analyzed.

On a set of healthy subjects who underwent naturalistic audio-visual stimulation, we demonstrate the usefulness of the approach by tying the unraveled functional reconfigurations to particular cues of the movie. We show how, through our method, one can capture either a temporal profile of brain activity (the evolution of a given connection), or focus on a spatial snapshot at a key time point. We provide a publicly available version of the whole pipeline, and describe its use and the influence of its key parameters step by step.

INTRODUCTION:

Functional magnetic resonance imaging (fMRI) has become the tool of choice to non-invasively monitor the changes in brain activity resulting from external stimulation. More specifically, vivid interest has emerged about the understanding of statistical interdependence between regional activation time courses, known as *functional connectivity* (FC)[1] and typically computed as Pearson's correlation coefficient. Functional interplays across the brain have been extensively shown to reconfigure as a function of the underlying task[2-4].

Two analytical directions have separately been followed to go beyond this introductory characterization: on the one hand, the response induced in a given brain region by a time-locked stimulus was observed to strongly correlate across distinct subjects[5]. Quantifying this *inter-subject correlation* (ISC) showed potential to refine our understanding of cognition[6-9] and brain disorders[10,11]. Further, this cross-subject correlational approach was also extended to the assessment of cross-regional synchronicity[12], in what became known as the *inter-subject functional correlation* (ISFC) approach[13].

On the other hand, the dynamic flavor of FC reconfigurations started to receive increased attention (see Hutchison et al.[14], Preti, Bolton and Van De Ville[15], Gonzales-Castillo and Bandettini[16] for recent reviews on the resting-state and task-based sides of this question). In particular, whole-brain FC changes over time can be tracked through consecutive correlation measurements over a gradually shifted temporal sub-window[17,18], revealing additional insight in the context of behavioral tasks[19,20].

Here, we present a methodological framework that combines those two avenues. Indeed, we compute ISFC in sliding-window fashion to track the evolution of cross-regional synchronicity between the subjects exposed to a time-locked, naturalistic paradigm. Through the cross-subject aspect of the method, analyses are focused on stimulus-driven effects, while spontaneous fMRI changes (which are uncorrelated across subjects) are strongly damped. This is important because resting-state and task-evoked activity patterns are increasingly understood to be characterized by distinct properties[21,22].

As for the dynamic component of the method, it enables a more complete and accurate characterization of task stimuli, particularly when probing a naturalistic paradigm in which a diverse set of cues (auditory, visual, social, etc.) are combined over time. Further, as the sound statistical evaluation of significant dynamic fluctuations has been hotly debated[23,24], our approach takes particular care of this aspect of the analyses by isolating significant ISFC changes through comparison to appropriate null data.

We illustrate the method on a set of healthy subjects exposed to an audio-visual movie stimulus, for whom we show that the temporal and spatial ISFC change profiles arising from localized movie sub-intervals can be accurately extracted. In doing so, we also describe the influence of the main analytical parameters to be selected by the user. The presented findings are based on part of formerly published data[25,26].

PROTOCOL:

The following protocol has been approved by the local ethics committee (Biomedical Inserm 365 protocol C08-39).

1. Pre-imaging

1.1. Enroll a study population of subjects, obtaining written, informed consent for all of them. Seek approval from the local ethics committee.

1.2. Select a paradigm to investigate that can be applied to all subjects in time-locked manner.

NOTE: Here, we used an audio-visual scientific documentary for youngsters (https://miplab.epfl.ch/index.php/miplife/research/supplement-asd-study).

2. Imaging

2.1. For each subject to consider in the analyses, perform at least one functional imaging session in which the scanned volunteer is subjected to the time-locked paradigm of interest.

2.1.1. Use a 3 Tesla MRI scanner to acquire transverse slices through an echoplanar imaging sequence.

2.1.2. Employ the following imaging parameters: voxel size = 3 mm x 3 mm x 3 mm, repetition time (TR) = 2 s, echo time = 50 ms, field of view = 192, 40 slices.

NOTE: Faster TR values are encouraged within the scope of feasibility. The protocol can also be applied with a more restricted field of view (e.g., for analyses restricted to a specific brain sub-structure), which would enable either a better temporal resolution (lower TR), or a spatially more precise analysis.

2.1.3. Leave a few seconds of recording (≥ 2 TR) before and after the presentation of the stimulus.

2.2. Perform at least one separate functional imaging session in which the scanned volunteer lies at rest in the scanner, eyes closed and instructed not to fall asleep.

NOTE: Separate stimulus-related and resting-state acquisitions prevent otherwise possible interplays between the conditions (e.g., having watched the movie beforehand may leave a lasting trace to a subsequently acquired resting-state recording)[27]. If it is not desired to go through the aforementioned additional resting-state acquisition, an alternative (albeit more prone to the detection of false positives; see Discussion) computational option in the pipeline replaces this data by surrogate time courses computed from the paradigm-related signals (see step 5.1.2).

2.3. Perform structural imaging.

2.3.1. Use a 3 Tesla MRI scanner and a T1-weighted magnetization-prepared rapid acquisition gradient echo sequence.

2.3.2. Employ the following imaging parameters: voxel size = 1 mm x 1 mm x 1 mm, field of view = 256, 176 slices.

3. Data and software preparation

3.1. For each session to analyze, ensure the existence of the following data files:

3.1.1. A set of functional MRI volumes, present as separate 3D NIFTI or HDR/IMG files, with a consistent numbering scheme (e.g., "fMRI_0001", "fMRI_0002", etc.).

3.1.2. A T1 structural MRI image, in NIFTI or HDR/IMG format.

3.1.3. An atlas of interest in Montreal Neurological Institute (MNI) space, in NIFTI format.

NOTE: An example of required input files is provided for a representative subject ("S17"), along with the full pipeline code, at **ssh://git@c4science.ch/source/Intersubj_pipeline.git**.

3.2. Download the latest version of the publically available Freesurfer software[28] (**https://surfer.nmr.mgh.harvard.edu/fswiki/DownloadAndInstall**).

3.3. Download the latest version of the publically available Statistical Parametric Mapping (SPM) MATLAB toolbox from **https://www.fil.ion.ucl.ac.uk/spm/software/spm12/**.

3.4. Open MATLAB (version 2017a or more recent) and locate the newly downloaded "freesurfer" and "spm12" folders. For each, right click on it and select the **Add to Path > Selected Folders and Subfolders** option.

4. Data preprocessing

4.1. In the MATLAB terminal, type **spm** to launch the SPM12 main menu, and click on the **fMRI** button to access the preprocessing options devoted to fMRI data. Perform the following steps separately for each fMRI session to preprocess.

4.1.1. Click on **Realign (Est & Res)**, and in the newly open Batch Editor window, double click on **Data** > **Session**. In the newly open Session window, select all functional images to process. Then, click on the **Done** button, and afterwards, on the **Run Batch** icon from the Batch Editor window (green triangle). Wait until the realignment step finishes, as indicated in the MATLAB terminal window.

4.1.2. Click on **Coregister (Est & Res)**, and in the newly open Batch Editor window, double click on **Reference image**. In the newly open Reference Image window, select the average functional volume created in the following step, prefixed with "mean", and click on the **Done** button. Then, double click on **Source image**, and in the newly open Source Image window, select the T1 image. Click on the **Done** button, and afterwards, on the **Run Batch** icon from the Batch Editor window (green triangle). Wait until the coregistration step finishes, as indicated in the MATLAB terminal window.

NOTE: The T1 image is overwritten at this step, so that the updated one lies in the same space as the functional volumes.

4.1.3. Click on **Segment**, and in the newly open Batch Editor window, double click on **Volumes**. In the newly open Volumes window, select the T1 image, and click on the **Done** button. Then, in the Batch Editor window, double click on **Deformation Fields** and select the **Inverse** option. Click on the **Run Batch** icon (green triangle), and wait until the segmentation step finishes, as indicated in the MATLAB terminal window.

4.2. Type **JOVE_GUI1** in the MATLAB terminal to open the first preprocessing graphical user interface window. Perform the following steps for each fMRI session to analyze.

4.2.1. Click on **Enter fMRI data**, and select all realigned functional volumes created in step 4.1.1 (prefixed with "r"). For IMG/HDR files, select both the IMG and HDR volumes.

4.2.2. Enter the TR of the data (in seconds) in the dedicated editable text window.

4.2.3. Click on **Enter T1 data** and select the three probabilistic tissue type volumes created in step 4.1.3 (prefixed with "c1", "c2" and "c3").

4.2.4. Click on **Enter motion file**, and select the text file containing motion parameters from the session of interest, created in step 4.1.3 and prefixed with "rp".

4.2.5. Select the desired type of preprocessing, that is, whether the data should be detrended or not (respectively setting the dedicated radio button on or off), and what covariates should be regressed out (by selecting the appropriate option from the dedicated list).

NOTE: The regression step is inspired from a function originating from the DPARSFA toolbox[29]. The white matter and cerebrospinal fluid signals from individual subjects are averaged over the voxels for which the respective template DPARSFA probabilistic tissue map showed a signal larger than 0.99. In our analyses, we detrended the data, and regressed out white matter/cerebrospinal fluid time courses as well as constant, linear and quadratic trends.

4.2.6. To preprocess the data, click on **Preprocess**, and wait for the display to appear in the window. The data can be re-preprocessed differently by modifying the options, and clicking again on the **Preprocess** button.

NOTE: The gray matter plot is inspired from the representation suggested by Power et al.[30].

[Place Supplementary **Figure 1** here]

4.2.7. To save the output for following steps, click on the **Save** button. To clear the content of the window, click on the **Clear** button.

4.3. Type **JOVE_GUI2** in the MATLAB terminal to open the second preprocessing graphical user interface window. Perform the following steps for each fMRI session to analyze.

4.3.1. Click on **Select data**, and select the data file saved in step 4.2.7 (named "ISFC_VX.mat").

4.3.2. Click on **Select motion**, and select the text file containing motion parameters from the session of interest, created in step 4.1.1 and prefixed with "rp".

4.3.3. Click on **Select atlas**, and select the NIFTI file representing the atlas to use for parcellation.

4.3.4. Click on **Select inverse warp**, and select the NIFTI file representing the deformation field from MNI to native space, created in step 4.1.1 and prefixed with "iy".

4.3.5. Click on **Select fMRI volume**, and select any of the fMRI data volumes.

NOTE: This step enables to access the header information of the functional data, hence why the actual chosen volume is not important.

4.3.6. Enter the TR of the data (in seconds) in the dedicated editable text window.

4.3.7. Enter scrubbing-related information: the type of scrubbing to perform (i.e., how many frames to scrub out before and after the tagged ones) in the "Scrubbing type" list, and the framewise displacement threshold value (Power's criterion[31]) above which an fMRI volume should be scrubbed in the "Scrubbing threshold" editable text window (in mm).

NOTE: Cubic spline interpolation is performed on the scrubbed data points to replace them with estimated values from neighboring samples. In our analyses, we scrubbed one frame after the tagged volumes, and used a 0.5 mm threshold for scrubbing.

4.3.8. Enter the size of the sliding-window W to use for ISFC computations (see step 5), in TRs.

NOTE: This piece of information will enable filtering of the time courses through a function originating from the DPARSFA toolbox[29], at f = 1/W Hz[32]. In our analyses, we used W = 10 TR as a trade-off value to capture dynamic fluctuations while conserving enough samples for robust estimations.

4.3.9. Click on the **Plot** button to display indicative atlased time courses before (top plot) and after (bottom plot) the scrubbing and filtering steps. Verify, by visual inspection, that following the selected preprocessing steps, those output signals do not incorporate salient artifactual components.

[Place Supplementary **Figure 2** here]

4.3.10. To save the outputs for following steps, enter a save name in the dedicated editable text window, and click on the **Save** button. To clear the content of the window, click on the **Clear** button.

5. Sliding-window ISFC computations

5.1. Type **JOVE_GUI3** in the MATLAB terminal to open the first ISFC-related graphical user interface window. Perform the following steps separately for each type of acquired fMRI session segment (stimulus-related segments, resting-state segments of stimulus-related sessions, and purely resting-state segments).

5.1.1. Click on **Load data**, and select all the appropriate data files created through step 4.3.

5.1.2. Select whether the selected session segments should undergo phase randomization.

NOTE: Phase randomization can be used as an alternative option for the generation of null data from stimulus-related signals, if no resting-state recordings are available.

5.1.3. Enter the TR of the data (in seconds) in the dedicated editable text window.

5.1.4. Enter sliding-window parameters to use for the analysis in the dedicated editable text windows: window size (in TRs) over which connectivity measurements should be computed, and step size (in TRs) by which successive windows should be shifted.

NOTE: In our analyses, we used a window size of 10 TR and a step size of 1 TR.

5.1.5. Modify the "Session types" table to specify which of the loaded session segments were acquired upon the same experimental condition. Use increasing integer numbers from 1 onwards to tag different types of segments (e.g., if the stimulus was displayed for the first or for the second time in a given recording). Leave the table untouched if only one type of session segment was acquired.

NOTE: A session in the present work may refer either to a combined movie/resting-state recording (termed RUN_1 and RUN_2 in **Figure 1A**), or to a purely resting-state recording (RUN_3). A session segment refers to a sub-portion of a session recording, either when the movie was watched, or when the subjects lied at rest. The above information is used in the subsequently described ISFC computations (see step 5.1.7) to limit the confounding influence of different session segment types.

5.1.6. Enter bootstrapping-related parameters in the dedicated editable text windows: the number of bootstrapping folds over which to perform ISFC computations, and the number of subjects that should constitute the reference group for each fold of ISFC computations.

NOTE: In our analyses, we used 250 bootstrapping folds, and 6 subjects into the reference group.

5.1.7. Enter specifications about which sub-portion of time courses should be analyzed in the **Timing parameters** section, in the dedicated editable text windows. A start index and an end index (in TRs) should be provided. To analyze the whole recording duration, use 1 as start index and the number of samples as end index.

5.1.8. Click on the **Plot** button to perform ISFC computations. Displays are gradually updated over time, along with the amount of elapsed bootstrapping folds. For a region pair (i,j) and a sliding window index τ, ISFC is computed as the average of cross-correlations between session segment s and all session segments from the reference group, within a sliding-window of length W; denote this reference group by Ψ, its number of subjects by N_Ψ, and let $x_i^{[s]}(t)$ the time course of region i for session segment s at time t; an ISFC estimate is then given by:

$$ISFC_{ij}^{[s]}(\tau) = \frac{\sum_{k\in\Psi} \rho(\boldsymbol{x_i^{[s]}}(\boldsymbol{t}:\boldsymbol{t}+\boldsymbol{W}), \boldsymbol{x_j^{[k]}}(\boldsymbol{t}:\boldsymbol{t}+\boldsymbol{W}))}{N_\Psi}.$$

ISFC measurements are computed over the specified amount of bootstrapping folds, and with the selected number of session segments used as a reference group at each fold (see step 5.1.6). If several session segment subtypes are included, a mixture of subtype samples always composes the reference group. The final output for each session segment is the average ISFC across all folds in which it was not included as a reference measurement.

NOTE: The reference group is the set of session segments to which the functional time courses of session segment s are compared at each fold of the bootstrapping process. For the results to be more robust to outlier data points, ISFC is computed multiple times on a different reference

group (that is, a different subset of session segments). Importantly, the acquisition time t does not match the sliding window index τ, as the latter is computed over a set of W data points, and relies on the window step size for successive estimates. The bootstrapping process was inspired from a former study by Byrge et al.[33].

[Place Supplementary **Figure 3** here]

5.1.9. To save the outputs for following steps, enter a save name in the dedicated editable text window, and click on the **Save** button. To clear the content of the window, click on the **Clear** button.

5.2. Type **JOVE_GUI4** in the MATLAB terminal to open the second ISFC-related graphical user interface window.

5.2.1. Click on **Load ISFC data** and select the stimulus-related ISFC output file(s) created in step 5.1.

5.2.2. Click on **Load null data** and select the resting-state ISFC output file(s) created in step 5.1.

5.2.3. Click on **Load codebook** and select the codebook file created in step 4.3.

5.2.4. Enter the TR of the data (in seconds) in the dedicated editable text window.

5.2.5. Enter the sliding-window parameters used in the computations of step 5.1 (window size and step size, in TRs) in the dedicated editable text windows.

5.2.6. Enter (in percent) the α-value at which the ISFC time courses should be thresholded to highlight significant changes in the dedicated editable text window.

NOTE: Here and elsewhere, when referring to an α-value of 2.5%, it means that significance is achieved when a value is lower than the 2.5th percentile, or larger than the 97.5th percentile, of the null data. In our analyses, we had 5,762 resting-state data points to our disposal, and selected an α-value of 10^{-4}. This means that we wanted 0.01% of data samples to be larger or equal to the selected thresholds past which an ISFC excursion would be deemed significant. For comparison purposes, the α-level demanded by Bonferroni correction would be 0.05/44,551 = 1.12 x 10^{-6}, and the most stringent possible α-level enabled with our amount of data (n samples) would be $\frac{1}{2n+2} = 8.68 \times 10^{-5}$.

5.2.7. Click on the **Plot** button to perform the ISFC thresholding process, in which all available resting-state ISFC measurements are aggregated, for a given connection, to construct a null distribution, following which stimulus-related ISFC measurements are thresholded according to the selected α-value. Time points at which a stimulus-related ISFC value statistically significantly

exceeds the null distribution are tagged as -1/+1 for significant ISFC decreases and increases, respectively.

NOTE: The thresholding process draws inspiration from the resting-state dynamic FC work of Betzel et al.[23].

5.2.8. To visualize the ISFC spatial patterns at different time points, drag the slider below the ISFC excursion plot.

[Place Supplementary **Figure 4** here]

REPRESENTATIVE RESULTS:

Here, we considered n = 15 typically developing (TD) subjects for whom we obtained written, informed consent. All were right-handed males (23.42 ± 7.8 years old). The chosen paradigm was an audio-visual scientific documentary for youngsters about the dangers of sun exposure. It contains a large array of visual, auditory and social stimuli, and can be watched at **https://miplab.epfl.ch/index.php/miplife/research/supplement-asd-study**.

We acquired two sessions per subject (RUN_1 and RUN_2) in which the assessed movie was displayed from 5 to 353 s (5.8 min duration). A resting-state segment also followed from 386 to 678 s (4.9 min duration). In addition, one solely resting-state session (RUN_3) was acquired for each subject (excluding one who suffered from claustrophobia), lasting for 310 s (5.2 min). Example movie scenes and the timing of acquired data are summarized in **Figure 1A**. Importantly, the acquisition protocol was not optimal in the sense that resting-state recordings acquired just after movie exposure may be partly corrupted by spillover effects[27]; we make use of this data in the present findings to have a satisfying amount of samples for statistical thresholding, but this should be avoided whenever possible.

We excluded all sessions for which more than 10% of frames were scrubbed, at a threshold of 0.5 mm, and considered the parcellation from Craddock et al.[34] (*two-level temporal correlation* algorithm) to generate regional time courses, for a total of 299 different brain regions.

ISFC was computed separately on (1) the movie-watching subparts of RUN1 and RUN_2, (2) the resting-state subparts of RUN_1 and RUN_2, and (3) the resting-state RUN_3 recordings. We used a window length W = 10 TR for the main presented results, and compare them to a lower value of W = 5 TR. Step size always remained equal to 1 TR. Bootstrapping was performed over 250 folds, including 6 session segments in each reference group.

Figure 1B displays ISFC time courses generated at W = 10 TR and W = 5 TR for three different representative connections: connection 1 involved a left inferior parietal region related to the expectation of moving objects (MNI coordinates: 41,9,32)[35], and a right frontal opercular area linked to response inhibition (-34,-52,45)[36]. This latter region was also implicated in connections 2 and 3, respectively with an area implicated in sensory coordination (54,6,34)[37], and one tied to the processing of the meaning of words (6,62,9)[38].

A comparison across window lengths reveals that in the W = 5 TR setting, temporal variance in the subjects is overall larger in both the movie-watching and resting-state segment cases as compared to W = 10 TR, a known phenomenon in sliding-window analyses[39]. For connection 1, regardless of the window length, a localized subpart of the movie-watching recording (at around 55 s) shows a strong, synchronized ISFC increase across subjects, which largely exceeds the range of values taken in the resting-state case. Thus, we expect to capture this temporal subpart as a significant ISFC transient with our thresholding method.

For connection 2, we observe similar temporal dynamics, but for W = 5 TR, the increase becomes less easy to disentangle as compared to the resting-state time courses, due to the larger sliding-window methodology-related noise. As for connection 3, it reflects a case in which there is no clear response to the movie, and thus, the fluctuations from movie-watching and resting-state time courses are similar. The expected outcome at this analytical stage is a mix between connections that show clear stimulus-induced reconfigurations, and connections that do not respond.

[Place **Figure 1** here]

Figure 2A displays the results following statistical thresholding of ISFC time courses, for the same three connections as above. A time course value of 1 means that all subjects underwent the same ISFC increase at the same time point; a value of 0 means that no subject underwent a significant ISFC change; a value of -1 represents a synchronous ISFC decrease across all subjects. As before, we contrast W = 5 TR and W = 10 TR, and we also highlight two α-value cases: α = 0.01%, and α = 5%.

Fitting with the above observations, a lower window length reduces the amount of extracted significant ISFC changes. For connection 1, both W = 5 TR and W = 10 TR, however, extract the same particular moment (t = 55 s) as showing a strong ISFC increase. Taking a hemodynamic delay of roughly 5 s into account, this corresponds to a subpart of the movie when colored lines were extending towards a doll, and abruptly stopped just in front of it (46-49 s), fitting with the role of the involved regions in moving object expectation and response inhibition[35,36].

When increasing α from 0.01% to 5%, one can observe a much lower specificity of the detected ISFC transients, likely including many false positives and expectedly showing much less temporal synchrony.

As another perspective that can be set on the data, **Figure 2B** shows the whole-brain spatial maps of significant ISFC changes at t = 55 s. It can be seen that the response to the movie scene extends far beyond the example connections described here.

[Place **Figure 2** here]

FIGURE AND TABLE LEGENDS:

Figure 1: Acquisition timing and example ISFC time courses. (**A**) The movie watched by the subjects involved a wide array of social situations (example images 1 and 4), scientific explanations with colorful panels (example images 2 and 5), and landscape sceneries (example image 3). Three sessions were acquired per subject: two (RUN_1 and RUN_2) included the movie stimulation (from 5 to 353 s, highlighted in green) followed by a resting-state period (from 386 to 678 s, shown in yellow), while one (RUN_3) solely consisted in a resting-state recording (310 s duration, displayed in orange). (**B**) For three indicative connections (C1, C2 and C3, respectively dark green/red, light green/orange and turquoise/yellow traces), evolution of ISFC over time during movie-watching (cold colors) or resting-state (hot colors). For W = 10 TR (left panel), movie-watching ISFC changes more largely stand out as compared to W = 5 TR (right panel). Each trace reflects the ISFC time course of one session. This figure has partly been modified from Bolton et al.[25].

Figure 2: Temporal and spatial snapshots of ISFC patterns. (**A**) ISFC transient time courses, averaged across subjects, for three indicative connections (C1, C2 and C3, respectively dark green, light green and turquoise traces). The movie scene that drove the ISFC changes is highlighted in light grey, and depicted by example images. For W = 10 TR (left column of plots), ISFC changes are more strongly detected than for W = 5 TR (right column of plots). For α = 0.01% (top row of plots), specificity to localized movie cues is larger than for α = 5% (bottom row of plots). Each trace reflects the ISFC transient time course of one session, and the two-tailed 95% confidence intervals are displayed as error measure. (**B**) For W = 10 TR and α = 0.01%, there is a neat, restricted spatial pattern of ISFC transients at t = 55 s (the peak ISFC transient value for C1); for W = 5 TR and α = 5%, connections undergoing a significant ISFC change at this time are much more numerous. Note that we assume a hemodynamic delay of around 5 s in the described temporality (i.e.,, a value of 55 s here relates to the movie stimulus at 50 s). This figure has partly been modified from Bolton et al.[25].

Supplementary Figure 1: Example screenshot from the first preprocessing graphical user interface window. Voxel-wise time courses of gray matter voxels following the selected preprocessing options (top right plot), and covariates that may be used in the preprocessing (from top to bottom: cerebrospinal fluid/white matter average time courses, translational motion parameters, and rotational motion parameters.

Supplementary Figure 2: Example screenshot from the second preprocessing graphical user interface window. Regional time courses following atlasing, before (top plot) and after (bottom plot) scrubbing and filtering according to selected parameters. Each curve depicts one regional time course randomly selected amongst all the available ones.

Supplementary Figure 3: Example screenshot from the first ISFC-related graphical user interface window. (Top plot) Schematic representation of how often each considered session has its ISFC measurements computed (i.e., is not selected within the reference group). (Bottom plot) On an indicative subject, ISFC time courses computed for fifty example connections, selected as the ones exhibiting the largest summed absolute ISFC values across time.

Supplementary Figure 4: Example screenshot from the second ISFC-related graphical user interface window. (Top left plot) On an indicative subject, ISFC time courses computed for three example connections, selected as the ones exhibiting the largest amount of significant ISFC excursions and displayed with their associated computed significance thresholds (horizontal lines). (Bottom left plot) For the same connections, associated excursion time courses averaged across subjects, with two-tailed 95% confidence intervals displayed as error measure. (Right plot) Spatial ISFC pattern (averaged ISFC excursions across subjects) for a selected time point indicated by a vertical black line on the ISFC and excursion plots. Positive ISFC excursions are shown in yellow, and negative ones in pink. The size and color code of the nodes are proportional to their degree.

Supplementary Figure 5: Detection of ISFC excursions across null data generation methods. For resting-state (left column, blue plots) or phase randomization (right column, red plots) null data generation methods, percentage of ISFC excursions extracted across connections. The bottom plots are an inset on the connections emanating from the first three considered brain regions. Error represents standard deviation across subjects.

DISCUSSION:

On a dataset of healthy subjects, we demonstrated how synchronous cross-subject increases and decreases in FC, the ISFC transients, would match temporally localized movie cues, providing information that goes beyond a static description. Although the use of cross-subject correlation measures enables to focus the analysis on stimulus-driven functional reconfigurations, one must also be aware that it limits the findings to the effects that are shared across the studied population: hence, low-level sensory processing is expected to be over-represented compared to frontal processing[40]. To bypass this limitation, new methods that also have the ability to extract the regions that most strongly vary across subjects are being developed[41].

Another limitation from the introduced methodology arises from the sliding-window aspect, as temporal resolution of ISFC transient time courses is lowered compared to frame-wise approaches[15]. As we showed, a trade-off is needed between a sufficiently low window length to properly resolve dynamic ISFC reconfigurations, and a large enough size to obtain robust estimates. Two critical steps in our framework ensure that the extracted ISFC transients reflect truly occurring changes in connectivity: first, the high-pass filtering of regional time courses with the inverse of the window length[32]; second, the use of resting-state ISFC data for the generation of a relevant null distribution, with identical acquisition parameters as compared to the stimulus-related data. Of course, the latter also requires a lengthier global acquisition time, so that resting-state data can be gathered on top of stimulus-related sessions. As an alternative approach to avoid the additional resting-state recordings, we also offer the possibility to generate phase randomized data directly from the stimulus-related time courses, an approach often used in dynamic functional connectivity analyses[23,24]. Further evaluation on a subset of sessions revealed that although the resting-state null method is more conservative, and thus

less prone to false positives, the global patterns of ISFC excursion detection were similar across both schemes (see **Supplementary Figure 5**).

[Place Supplementary **Figure 5** here]

The duration of the resting-state acquisitions actually relates to a critical parameter of the analyses: the α-value. As exemplified above, a too lenient choice will lead to a large amount of false positives in the detected ISFC transients. The larger the amount of available resting-state data, the more stringent the achievable false positive rate, because thresholding can be based on more extreme values from the null distribution. As an indication, for n = 299 atlas regions as here and given our tally of 5,762 resting-state data points, we could at best achieve an α-value close to 0.01% (see step 5.2.6 for mathematical details).

Another key point pertaining to any fMRI analysis lies in the rigorous removal of possible motion-related artifacts from the analyzed data[29,42]. In particular, if one wishes to apply the introduced pipeline to diseased populations exhibiting marked motion in the scanner, we recommend that on top of including motion variables as covariates in the performed statistical analyses, additional preprocessing steps be run, such as wavelet denoising[43] or ICA-AROMA[44]. Group comparison, for instance to compare ISFC transients between a healthy and a diseased group, can readily be performed by running the described approach in parallel on both groups of interest (see Bolton et al.[25] for an example on a population diagnosed with autism spectrum disorders). However, a difference between the groups can then arise in two distinct settings: (1) an absent ISFC change in one group, or (2) a more heterogeneous evolution in that group. To disentangle those two factors, the pipeline should be run once more for the diseased group, using the healthy subject set as the reference group at the bootstrapping step. The former case would still result in an absent response, whereas the latter would not.

On top of what we described here, the introduced methodology also opens up promising future avenues: from an analytical side, ISFC transient maps could be viewed as brain graphs from which metrics quantifying brain connectivity could be derived[45], or dynamic ISFC states could be extracted through clustering approaches and assessed in terms of their spatial and temporal characteristics[18,46]. In addition, one could also envisage the use of more sophisticated connectivity measurement tools than Pearson's correlation coefficient to reveal subtler sides of FC[47,48].

From the experimental side, the application of our pipeline to a more extended set of paradigms is a promising perspective: for example, instead of a movie as studied here, one could envisage to use a piece of music[49] or a narrative story[13,50] as a time-locked stimulus. Alternatively, it could even be envisioned, through hyperscanning[51], to probe naturalistic social communication[52,53].

ACKNOWLEDGMENTS:
This work was supported in part by each of the following: the Swiss National Science Foundation (grant number 205321_163376 to DVDV), the Bertarelli Foundation (to TB and

DVDV), the Center for Biomedical Imaging (CIBM), and the National Agency for Research (tempofront grant number 04701 to ALG).

DISCLOSURES:

The authors have nothing to disclose.

REFERENCES:

1. Friston, K.J. Functional and effective connectivity in neuroimaging: A synthesis. *Human Brain Mapping*. **2** (1-2), 56-78 (1994).

2. Gonzales-Castillo, J. et al. Tracking ongoing cognition in individuals using brief, whole-brain functional connectivity patterns. *Proceedings of the National Academy of Sciences U.S.A.* **112** (28), 8762-8767 (2015).

3. Peltz, E. et al. Functional connectivity of the human insular cortex during noxious and innocuous thermal stimulation. *Neuroimage*. **54** (2), 1324-1335 (2011).

4. Shirer, W.R., Ryali, S., Rykhlevskaia, E., Menon, V., Greicius, M.D. Decoding subject-driven cognitive states with whole-brain connectivity patterns. *Cerebral Cortex*. **22** (1), 158-165 (2012).

5. Hasson, U., Nir, Y., Levy, I., Fuhrmann, G., Malach, R. Intersubject Synchronization of Cortical Activity During Natural Vision. *Science*. **303** (5664), 1634-1640 (2004).

6. Hasson, U., Furman, O., Clark, D., Dudai, Y., Davachi, L. Enhanced Intersubject Correlations during Movie Viewing Correlate with Successful Episodic Encoding. *Neuron*. **57** (3), 452-462 (2008).

7. Hasson, U., Yang, E., Vallines, I., Heeger, D.J., Rubin, N. A Hierarchy of Temporal Receptive Windows in Human Cortex. *Journal of Neuroscience*. **28** (10), 2539-2550 (2008).

8. Jääskeläinen, I.P. et al. Inter-Subject Synchronization of Prefrontal Cortex Hemodynamic Activity During Natural Viewing. *The Open Neuroimaging Journal*, **2**, 14 (2008).

9. Wilson, S.M., Molnar-Szakacs, I., Iacoboni, M. Beyond Superior Temporal Cortex: Intersubject Correlations in Narrative Speech Comprehension. *Cerebral Cortex*, **18** (1), 230-242 (2008).

10. Hasson, U. et al. Shared and idiosyncratic cortical activation patterns in autism revealed under continuous real-life viewing conditions. *Autism Research*, **2** (4), 220-231 (2009).

11. Salmi, J. et al. The brains of high functioning autistic individuals do not synchronize with those of others. *NeuroImage: Clinical*, **3**, 489-497 (2013).

12. Mantini, D. et al. Interspecies activity correlations reveal functional correspondence between monkey and human brain areas. *Nature Methods*, **9** (3), 277 (2012).

13. Simony, E. et al. Dynamic reconfiguration of the default mode network during narrative comprehension. *Nature Communications*, **7**, 12141 (2016).

14. Hutchison, R.M. et al. Dynamic functional connectivity: promise, issues, and interpretations. *Neuroimage*, **80**, 360-378 (2013).

15. Preti, M.G., Bolton, T.A.W., Van De Ville, D. The dynamic functional connectome: state-of-the-art and perspectives. *Neuroimage*, **160**, 41-54 (2017).

16. Gonzalez-Castillo, J., Bandettini, P.A. Task-based dynamic functional connectivity: Recent findings and open questions. *Neuroimage*, **180**, 526-533 (2018).

17. Allen, E.A. et al. Tracking whole-brain connectivity dynamics in the resting state. *Cerebral Cortex*, **24** (3), 663-676 (2014).

18. Sakoğlu, Ü. et al. A method for evaluating dynamic functional network connectivity and task-modulation: application to schizophrenia. *Magnetic Resonance Materials in Physics, Biology and Medicine*, **23** (5-6), 351-366 (2010).

19. Douw, L., Wakeman, D., Tanaka, N., Liu, H. State-dependent variability of dynamic functional connectivity between frontoparietal and default networks relates to cognitive flexibility. *Neuroscience*, **339**, 12-21 (2016).

20. Mooneyham, B.W. et al. States of mind: characterizing the neural bases of focus and mind-wandering through dynamic functional connectivity. *Journal of Cognitive Neuroscience*, **29** (3), 495-506 (2017).

21. Kim, D., Kay, K., Shulman, G.L., Corbetta, M. A New Modular Brain Organization of the BOLD Signal during Natural Vision. *Cerebral Cortex*, **28** (9), 3065-3081 (2018).

22. Lynch, L.K. et al. Task-Evoked Functional Connectivity Does Not Explain Functional Connectivity Differences Between Rest and Task Conditions. *Human Brain Mapping*, **39**, 4939-4948 (2018).

23. Betzel, R.F., Fukushima, M., He, Y., Zuo, X.N., Sporns, O. Dynamic fluctuations coincide with periods of high and low modularity in resting-state functional brain networks. *Neuroimage*, **127**, 287-297 (2016).

24. Hindriks, R. et al. Can sliding-window correlations reveal dynamic functional connectivity in resting-state fMRI? *Neuroimage*, **127**, 242-256 (2016).

25. Bolton, T.A.W., Jochaut, D., Giraud, A.L., Van De Ville, D. Brain dynamics in ASD during movie-watching show idiosyncratic functional integration and segregation. *Human Brain Mapping*, **39** (6), 2391-2404 (2018).

26. Jochaut, D. et al. Atypical coordination of cortical oscillations in response to speech in autism. *Frontiers in Human Neuroscience*, **9**, 171 (2015).

27. Dodero, L., Sona, D., Meskaldji, D.E., Murino, V., Van De Ville, D. Traces of human functional activity: Moment-to-moment fluctuations in fMRI data. *Biomedical Imaging (ISBI), 2016 IEEE 13th International Symposium*, 1307-1310 (2016).

28. Fischl, B. Freesurfer. *Neuroimage*, **62** (2), 774-781 (2012).

29. Yan, C., Zang, Y. DPARSF: a MATLAB toolbox for "pipeline" data analysis of resting-state fMRI. *Frontiers in Systems Neuroscience*, **4**, 13 (2010).

30. Power, J.D. et al. Methods to detect, characterize, and remove motion artifact in resting state fMRI. *Neuroimage*, **84**, 320-341 (2014).

31. Power, J.D., Barnes, K.A., Snyder, A.Z., Schlaggaer, B.L., Petersen, S.E. Spurious but systematic correlations in functional connectivity MRI networks arise from subject motion. *Neuroimage*, **59** (3), 2142-2154 (2012).

32. Leonardi, N., Van De Ville, D. On spurious and real fluctuations of dynamic functional connectivity during rest. *Neuroimage*, **104**, 430-436 (2015).

33. Byrge, L., Dubois, J., Tyszka, J.M., Adolphs, R., Kennedy, D.P. Idiosyncratic brain activation patterns are associated with poor social comprehension in autism. *Journal of Neuroscience*, **35** (14), 5837-5850 (2015).

34. Craddock, R.C., James, G.A., Holtzheimer III, P.E., Hu, X.P., Mayberg, H.S. A whole brain fMRI atlas generated *via* spatially constrained spectral clustering. *Human Brain Mapping*, **33** (8), 1914-1928 (2012).

35. Shulman, G.L. et al. Areas involved in encoding and applying directional expectations to moving objects. *Journal of Neuroscience*, **19** (21), 9480-9496 (1999).

36. Sebastian, A. et al. Disentangling common and specific neural subprocesses of response inhibition. *Neuroimage*, **64**, 601-615 (2013).

37. Oullier, O., Jantzen, K.J., Steinberg, F.L., Kelso, J.A.S. Neural substrates of real and imagined sensorimotor coordination. *Cerebral Cortex*, **15** (7), 975-985 (2004).

38. Chan, A.H. et al. Neural systems for word meaning modulated by semantic ambiguity. *Neuroimage*, **22** (3), 1128-1133 (2004).

39. Lindquist, M.A., Xu, Y., Nebel, M.B., Caffo, B.S. Evaluating dynamic bivariate correlations in resting-state fMRI: A comparison study and a new approach. *Neuroimage*, **101** (1), 531-546 (2014).

40. Ren, Y., Nguyen, V.T., Guo, L., Guo, C.C. Inter-subject functional correlation reveal a hierarchical organization of extrinsic and intrinsic systems in the brain. *Scientific Reports*, **7** (1), 10876 (2017).

41. Kauppi, J.P., Pajula, J., Niemi, J., Hari, R., Tohka, J. Functional brain segmentation using inter-subject correlation in fMRI. *Human Brain Mapping*, **38** (5), 2643-2665 (2017).

42. Van Dijk, K.R., Sabuncu, M.R., Buckner, R.L. The influence of head motion on intrinsic functional connectivity MRI. *Neuroimage*, **59** (1), 431-438 (2012).

43. Patel, A.X. et al. A wavelet method for modeling and despiking motion artifacts from resting-state fMRI time series. *Neuroimage*, **95**, 287-304 (2014).

44. Pruim, R.H. et al. ICA-AROMA: A robust ICA-based strategy for removing motion artifacts from fMRI data. *Neuroimage*, **112**, 267-277 (2015).

45. Rubinov, M., Sporns, O. Complex network measures of brain connectivity: uses and interpretations. *Neuroimage*, **52** (3), 1059-1069 (2010).

46. Damaraju, E. et al. Dynamic functional connectivity analysis reveals transient states of dysconnectivity in schizophrenia. *NeuroImage: Clinical*, **5**, 298-308 (2014).

47. Smith, S. et al. Network modelling methods for FMRI. *Neuroimage*, **54** (2), 875-891 (2011).

48. Meskaldji, D.E. et al. Prediction of long-term memory scores in MCI based on resting-state fMRI. *NeuroImage: Clinical*, **12**, 785-795 (2016).

49. Abrams et al. Inter-subject synchronization of brain responses during natural music listening. *European Journal of Neuroscience*, **37** (9), 1458-1469 (2013).

50. Huth, A.G., de Heer, W.A., Griffiths, T.L., Theunissen, F.E., Gallant, J.L. Natural speech reveals the semantic maps that tile human cerebral cortex. *Nature*, **532** (7600), 453 (2016).

51. Montague, P.R. et al. Hyperscanning: simultaneous fMRI during linked social interactions. *Neuroimage*, **16**, 1159-1164 (2002).

52. Bilek, E. et al. Information flow between interacting human brains: Identification, validation, and relationship to social expertise. *Proceedings of the National Academy of Sciences U.S.A.*, **112** (16), 5207-5212 (2015).

53. Kinreich, S., Djalovski, A., Kraus, L., Louzoun, Y., Feldman, R. Brain-to-brain synchrony during naturalistic social interactions. *Scientific Reports*, **7** (1), 17060 (2017).

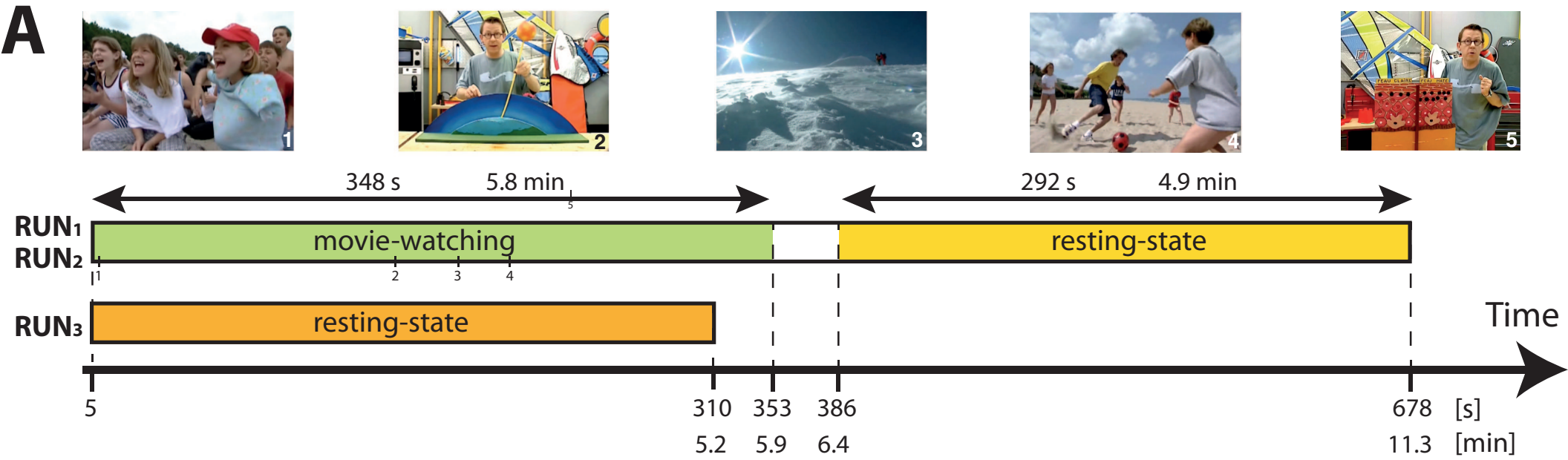

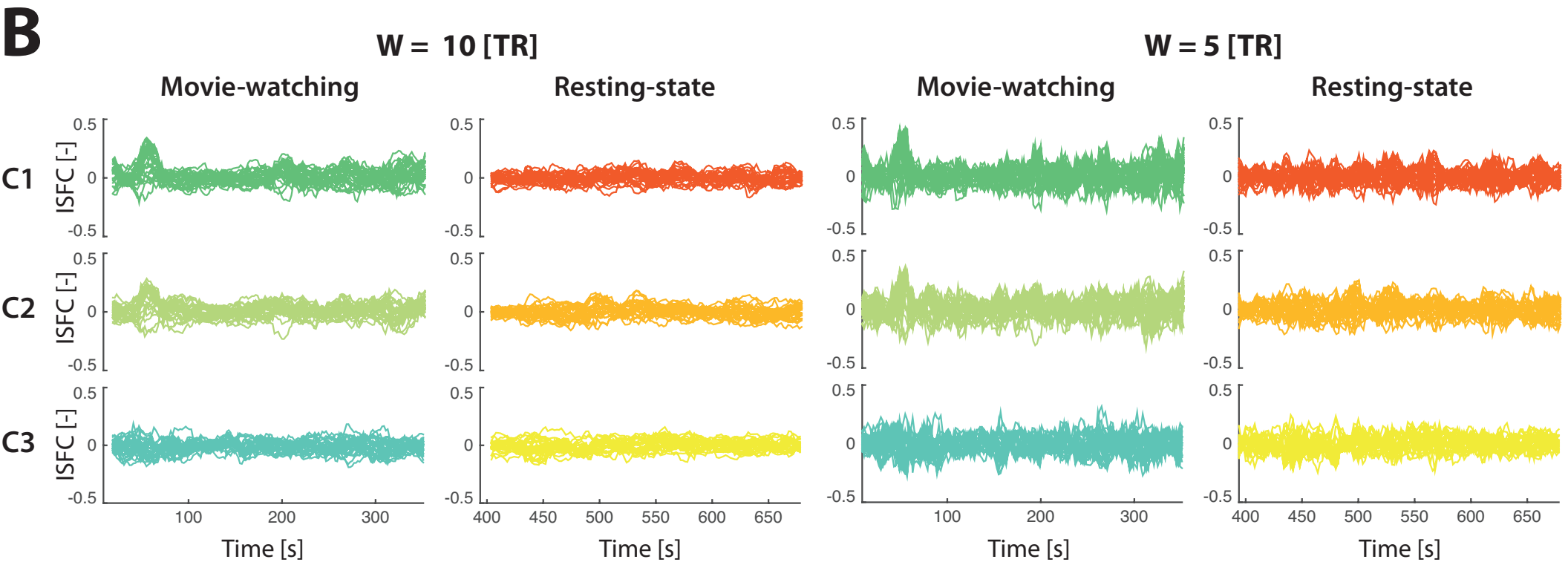

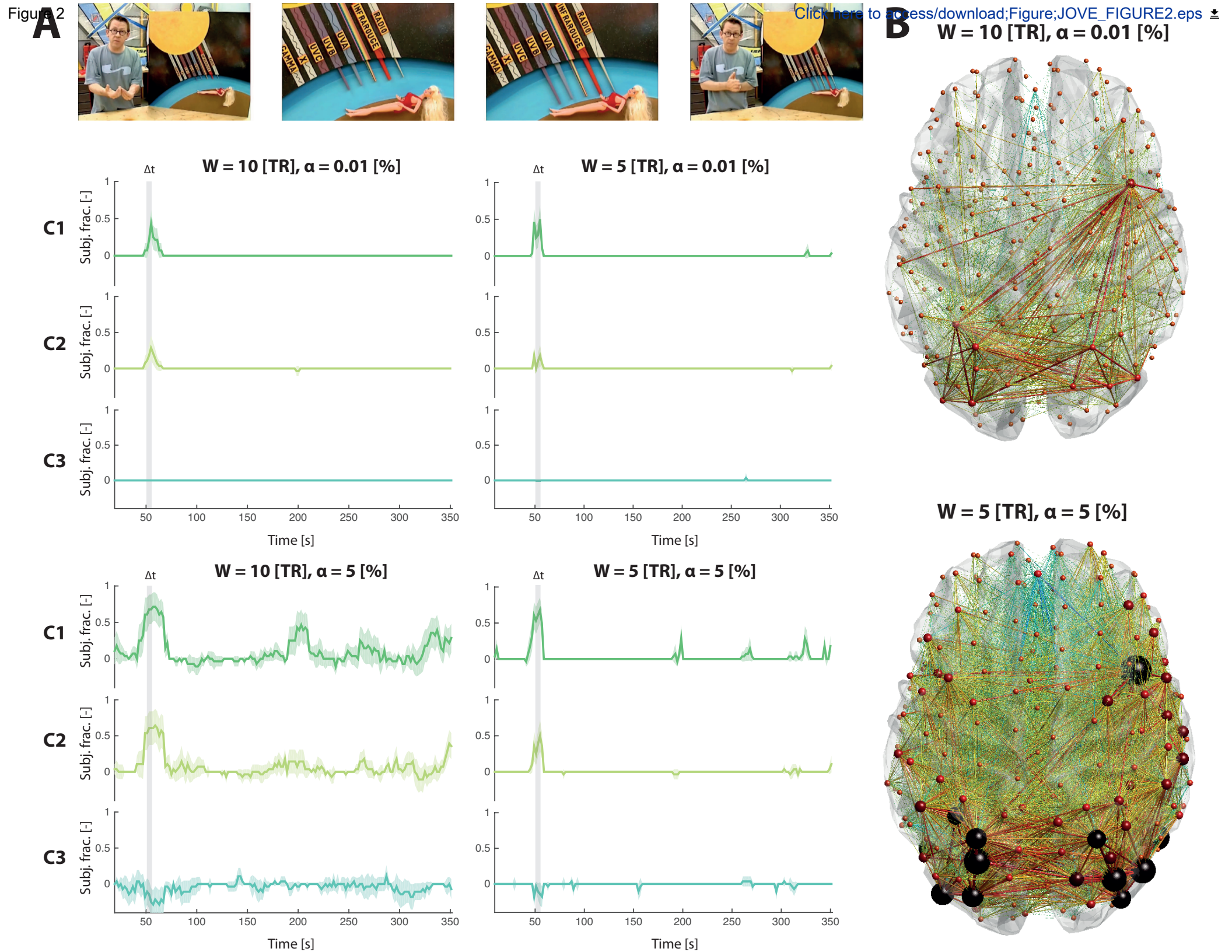

Table of Materials

Click here to access/download;Table of Materials;JoVE_Materials.xlsx

Name of Material/ Equipment
Freesurfer version 6.0
MATLAB_R2017a
Statistical Parametric Mapping version 12.0 (SPM12)
Tim-Trio 3 T MRI scanner

Company
Laboratory for Computational Neuroimaging, Martinos Center for Biomedical Imaging, Boston (MA), US
MathWorks
Wellcome Trust Center for Neuroimaging, University College London, London, UK
Siemens

Catalog Number
https://surfer.nmr.mgh.harvard.edu/fswiki/DownloadAndInstall https://ch.mathworks.com/downloads/ https://www.fil.ion.ucl.ac.uk/spm/software/spm12/ https://www.healthcare.siemens.ch/magnetic-resonance-imaging/for-installed-base-business-only-do-not-publi

Comments/Description
A MATLAB-compatible toolbox enabling to carry out various processing, visualisation and analytical steps on fun
Working version of the MATLAB computational software (version 2014a or more recent should be used)
A MATLAB-compatible toolbox enabling to perform statistical analyses on functional magnetic resonance imagin
Magnetic resonance imaging scanner in which subjects have their functional brain activity recorded (at 3 T)

ctional magnetic resonance imaging data

g data

jove JOURNAL OF VISUALIZED EXPERIMENTS
1 Alewife Center #200
Cambridge, MA 02140
tel. 617.945.9051
www.jove.com

ARTICLE AND VIDEO LICENSE AGREEMENT

Title of Article: Dynamic Inter-Subject Functional Connectivity Reveals Moment-to-Moment Brain Network Configurations Driven by Continuous or Communication Paradigms

Author(s): Thomas BOLTON, Delphine Jochaut, Anne-Lise Giraud, Dimitri Van De Ville

Item 1: The Author elects to have the Materials be made available (as described at http://www.jove.com/publish) via:

☐ Standard Access ☒ Open Access

Item 2: Please select one of the following items:

☒ The Author is **NOT** a United States government employee.

☐ The Author is a United States government employee and the Materials were prepared in the course of his or her duties as a United States government employee.

☐ The Author is a United States government employee but the Materials were NOT prepared in the course of his or her duties as a United States government employee.

ARTICLE AND VIDEO LICENSE AGREEMENT

1. **Defined Terms.** As used in this Article and Video License Agreement, the following terms shall have the following meanings: "**Agreement**" means this Article and Video License Agreement; "**Article**" means the article specified on the last page of this Agreement, including any associated materials such as texts, figures, tables, artwork, abstracts, or summaries contained therein; "**Author**" means the author who is a signatory to this Agreement; "**Collective Work**" means a work, such as a periodical issue, anthology or encyclopedia, in which the Materials in their entirety in unmodified form, along with a number of other contributions, constituting separate and independent works in themselves, are assembled into a collective whole; "**CRC License**" means the Creative Commons Attribution-Non Commercial-No Derivs 3.0 Unported Agreement, the terms and conditions of which can be found at: http://creativecommons.org/licenses/by-nc-nd/3.0/legalcode; "**Derivative Work**" means a work based upon the Materials or upon the Materials and other pre-existing works, such as a translation, musical arrangement, dramatization, fictionalization, motion picture version, sound recording, art reproduction, abridgment, condensation, or any other form in which the Materials may be recast, transformed, or adapted; "**Institution**" means the institution, listed on the last page of this Agreement, by which the Author was employed at the time of the creation of the Materials; "**JoVE**" means MyJove Corporation, a Massachusetts corporation and the publisher of The Journal of Visualized Experiments; "**Materials**" means the Article and / or the Video; "**Parties**" means the Author and JoVE; "**Video**" means any video(s) made by the Author, alone or in conjunction with any other parties, or by JoVE or its affiliates or agents, individually or in collaboration with the Author or any other parties, incorporating all or any portion of the Article, and in which the Author may or may not appear.

2. **Background.** The Author, who is the author of the Article, in order to ensure the dissemination and protection of the Article, desires to have the JoVE publish the Article and create and transmit videos based on the Article. In furtherance of such goals, the Parties desire to memorialize in this Agreement the respective rights of each Party in and to the Article and the Video.

3. **Grant of Rights in Article.** In consideration of JoVE agreeing to publish the Article, the Author hereby grants to JoVE, subject to **Sections 4** and **7** below, the exclusive, royalty-free, perpetual (for the full term of copyright in the Article, including any extensions thereto) license (a) to publish, reproduce, distribute, display and store the Article in all forms, formats and media whether now known or hereafter developed (including without limitation in print, digital and electronic form) throughout the world, (b) to translate the Article into other languages, create adaptations, summaries or extracts of the Article or other Derivative Works (including, without limitation, the Video) or Collective Works based on all or any portion of the Article and exercise all of the rights set forth in (a) above in such translations, adaptations, summaries, extracts, Derivative Works or Collective Works and(c) to license others to do any or all of the above. The foregoing rights may be exercised in all media and formats, whether now known or hereafter devised, and include the right to make such modifications as are technically necessary to exercise the rights in other media and formats. If the "Open Access" box has been checked in **Item 1** above, JoVE and the Author hereby grant to the public all such rights in the Article as provided in, but subject to all limitations and requirements set forth in, the CRC License.

jove JOURNAL OF VISUALIZED EXPERIMENTS
1 Alewife Center #200
Cambridge, MA 02140
tel. 617.945.9051
www.jove.com

ARTICLE AND VIDEO LICENSE AGREEMENT

4. **Retention of Rights in Article.** Notwithstanding the exclusive license granted to JoVE in **Section 3** above, the Author shall, with respect to the Article, retain the non-exclusive right to use all or part of the Article for the non-commercial purpose of giving lectures, presentations or teaching classes, and to post a copy of the Article on the Institution's website or the Author's personal website, in each case provided that a link to the Article on the JoVE website is provided and notice of JoVE's copyright in the Article is included. All non-copyright intellectual property rights in and to the Article, such as patent rights, shall remain with the Author.

5. **Grant of Rights in Video – Standard Access.** This **Section 5** applies if the "Standard Access" box has been checked in **Item 1** above or if no box has been checked in **Item 1** above. In consideration of JoVE agreeing to produce, display or otherwise assist with the Video, the Author hereby acknowledges and agrees that, Subject to **Section 7** below, JoVE is and shall be the sole and exclusive owner of all rights of any nature, including, without limitation, all copyrights, in and to the Video. To the extent that, by law, the Author is deemed, now or at any time in the future, to have any rights of any nature in or to the Video, the Author hereby disclaims all such rights and transfers all such rights to JoVE.

6. **Grant of Rights in Video – Open Access.** This **Section 6** applies only if the "Open Access" box has been checked in **Item 1** above. In consideration of JoVE agreeing to produce, display or otherwise assist with the Video, the Author hereby grants to JoVE, subject to **Section 7** below, the exclusive, royalty-free, perpetual (for the full term of copyright in the Article, including any extensions thereto) license (a) to publish, reproduce, distribute, display and store the Video in all forms, formats and media whether now known or hereafter developed (including without limitation in print, digital and electronic form) throughout the world, (b) to translate the Video into other languages, create adaptations, summaries or extracts of the Video or other Derivative Works or Collective Works based on all or any portion of the Video and exercise all of the rights set forth in (a) above in such translations, adaptations, summaries, extracts, Derivative Works or Collective Works and (c) to license others to do any or all of the above. The foregoing rights may be exercised in all media and formats, whether now known or hereafter devised, and include the right to make such modifications as are technically necessary to exercise the rights in other media and formats. For any Video to which this **Section 6** is applicable, JoVE and the Author hereby grant to the public all such rights in the Video as provided in, but subject to all limitations and requirements set forth in, the CRC License.

7. **Government Employees.** If the Author is a United States government employee and the Article was prepared in the course of his or her duties as a United States government employee, as indicated in **Item 2** above, and any of the licenses or grants granted by the Author hereunder exceed the scope of the 17 U.S.C. 403, then the rights granted hereunder shall be limited to the maximum rights permitted under such statute. In such case, all provisions contained herein that are not in conflict with such statute shall remain in full force and effect, and all provisions contained herein that do so conflict shall be deemed to be amended so as to provide to JoVE the maximum rights permissible within such statute.

8. **Protection of the Work.** The Author(s) authorize JoVE to take steps in the Author(s) name and on their behalf if JoVE believes some third party could be infringing or might infringe the copyright of either the Author's Article and/or Video.

9. **Likeness, Privacy, Personality.** The Author hereby grants JoVE the right to use the Author's name, voice, likeness, picture, photograph, image, biography and performance in any way, commercial or otherwise, in connection with the Materials and the sale, promotion and distribution thereof. The Author hereby waives any and all rights he or she may have, relating to his or her appearance in the Video or otherwise relating to the Materials, under all applicable privacy, likeness, personality or similar laws.

10. **Author Warranties.** The Author represents and warrants that the Article is original, that it has not been published, that the copyright interest is owned by the Author (or, if more than one author is listed at the beginning of this Agreement, by such authors collectively) and has not been assigned, licensed, or otherwise transferred to any other party. The Author represents and warrants that the author(s) listed at the top of this Agreement are the only authors of the Materials. If more than one author is listed at the top of this Agreement and if any such author has not entered into a separate Article and Video License Agreement with JoVE relating to the Materials, the Author represents and warrants that the Author has been authorized by each of the other such authors to execute this Agreement on his or her behalf and to bind him or her with respect to the terms of this Agreement as if each of them had been a party hereto as an Author. The Author warrants that the use, reproduction, distribution, public or private performance or display, and/or modification of all or any portion of the Materials does not and will not violate, infringe and/or misappropriate the patent, trademark, intellectual property or other rights of any third party. The Author represents and warrants that it has and will continue to comply with all government, institutional and other regulations, including, without limitation all institutional, laboratory, hospital, ethical, human and animal treatment, privacy, and all other rules, regulations, laws, procedures or guidelines, applicable to the Materials, and that all research involving human and animal subjects has been approved by the Author's relevant institutional review board.

11. **JoVE Discretion.** If the Author requests the assistance of JoVE in producing the Video in the Author's facility, the Author shall ensure that the presence of JoVE employees, agents or independent contractors is in accordance with the relevant regulations of the Author's institution. If more than one author is listed at the beginning of this Agreement, JoVE may, in its sole

jove VISUALIZED JOURNAL OF EXPERIMENTS
1 Alewife Center #200
Cambridge, MA 02140
tel. 617.945.9051
www.jove.com

ARTICLE AND VIDEO LICENSE AGREEMENT

discretion, elect not take any action with respect to the Article until such time as it has received complete, executed Article and Video License Agreements from each such author. JoVE reserves the right, in its absolute and sole discretion and without giving any reason therefore, to accept or decline any work submitted to JoVE. JoVE and its employees, agents and independent contractors shall have full, unfettered access to the facilities of the Author or of the Author's institution as necessary to make the Video, whether actually published or not. JoVE has sole discretion as to the method of making and publishing the Materials, including, without limitation, to all decisions regarding editing, lighting, filming, timing of publication, if any, length, quality, content and the like.

12. **Indemnification.** The Author agrees to indemnify JoVE and/or its successors and assigns from and against any and all claims, costs, and expenses, including attorney's fees, arising out of any breach of any warranty or other representations contained herein. The Author further agrees to indemnify and hold harmless JoVE from and against any and all claims, costs, and expenses, including attorney's fees, resulting from the breach by the Author of any representation or warranty contained herein or from allegations or instances of violation of intellectual property rights, damage to the Author's or the Author's institution's facilities, fraud, libel, defamation, research, equipment, experiments, property damage, personal injury, violations of institutional, laboratory, hospital, ethical, human and animal treatment, privacy or other rules, regulations, laws, procedures or guidelines, liabilities and other losses or damages related in any way to the submission of work to JoVE, making of videos by JoVE, or publication in JoVE or elsewhere by JoVE. The Author shall be responsible for, and shall hold JoVE harmless from, damages caused by lack of sterilization, lack of cleanliness or by contamination due to the making of a video by JoVE its employees, agents or independent contractors. All sterilization, cleanliness or decontamination procedures shall be solely the responsibility of the Author and shall be undertaken at the Author's expense. All indemnifications provided herein shall include JoVE's attorney's fees and costs related to said losses or damages. Such indemnification and holding harmless shall include such losses or damages incurred by, or in connection with, acts or omissions of JoVE, its employees, agents or independent contractors.

13. **Fees.** To cover the cost incurred for publication, JoVE must receive payment before production and publication the Materials. Payment is due in 21 days of invoice. Should the Materials not be published due to an editorial or production decision, these funds will be returned to the Author. Withdrawal by the Author of any submitted Materials after final peer review approval will result in a US$1,200 fee to cover pre-production expenses incurred by JoVE. If payment is not received by the completion of filming, production and publication of the Materials will be suspended until payment is received.

14. **Transfer, Governing Law.** This Agreement may be assigned by JoVE and shall inure to the benefits of any of JoVE's successors and assignees. This Agreement shall be governed and construed by the internal laws of the Commonwealth of Massachusetts without giving effect to any conflict of law provision thereunder. This Agreement may be executed in counterparts, each of which shall be deemed an original, but all of which together shall be deemed to me one and the same agreement. A signed copy of this Agreement delivered by facsimile, e-mail or other means of electronic transmission shall be deemed to have the same legal effect as delivery of an original signed copy of this Agreement.

A signed copy of this document must be sent with all new submissions. Only one Agreement is required per submission.

CORRESPONDING AUTHOR

Name:	Thomas BOLTON
Department:	Institute of Bioengineering
Institution:	École Polytechnique Fédérale de Lausanne
Title:	Mr
Signature:	Th Bolt
Date:	25.07.2018

Please submit a **signed** and **dated** copy of this license by one of the following three methods:

1. Upload an electronic version on the JoVE submission site
2. Fax the document to +1.866.381.2236
3. Mail the document to JoVE / Attn: JoVE Editorial / 1 Alewife Center #200 / Cambridge, MA 02140

Responses to Reviewers and Editor

We would like to thank both Reviewers and the Editor for their precious feedback about our submitted article. We have reworked our manuscript to incorporate all the required modifications, and below, we provide point-by-point answers to their different points.

Editor

1. Please take this opportunity to thoroughly proofread the manuscript to ensure that there are no spelling or grammar issues. The JoVE editor will not copy-edit your manuscript and any errors in the submitted revision may be present in the published version.

We have performed an extensive proofreading of the article, to ensure that there were no left grammatical or spelling mistakes.

2. Figure 1: Please include a space between the number and the unit: 348 s instead of 348s, etc.

Figure 1 has been modified to add a space wherever required between numbers and associated units: namely, '348s' was changed into '348 s', '5.8min' into '5.8 min', '292s' into '292 s', and '4.9min' into '4.9 min'.

3. Please revise the table of the essential supplies, reagents, and equipment. The table should include the name, company, and catalog number of all relevant materials in separate columns in an xls/xlsx file.

According to the Editor's suggestion, we have improved the table of essential supplies: on top of verifying the proper layout of the final file, we ensured that all required columns were properly filled in. For the described materials, a catalog number was not available; instead, we filled the entry with a link for downloading the related software, or towards the description of the product on its dedicated website.

4. Please include an ethics statement before the numbered protocol steps, indicating that the protocol follows the guidelines of your institution's human research ethics committee.

A sentence has now been added before numbered protocol steps, to specify that presented steps comply with the local ethics committee rules:

"The following protocol has been approved by the local ethics committee (Biomedical Inserm 365 protocol C08-39)."

To avoid redundancy, we also removed the related sentence initially present at the start of the Representative Results section.

5. Please add more details to your protocol steps. Please ensure you answer the "how" question, i.e., how is the step performed? Alternatively, add references to published material specifying how to perform the protocol action.

In accordance with the Editor's suggestion, we have thoroughly screened the article to ensure that every methodological step was properly described, and added details wherever required. Our additions can be read in red font throughout the updated manuscript document.

6. 2.5: How is structural imaging done?

To clarify Section 2 from the Protocol and thus answer the Editor's request, we modified it to merge information about structural/functional imaging parameters (previously given in Sections 2.1 and 2.2) within the experimental step sub points *per se* (previously Sections 2.3 to 2.5). The newer section version is, we hope, more homogeneous and clearer for someone wishing to replicate our protocol.

7. Please specify the computational parameters (specific values) used in the protocol. It is best to film a specific example instead of a generalized one.

We thank the Editor for his valuable comment. Accordingly, we now explicitly specify the parameters used in our Representative Results section within the protocol itself, in dedicated protocol notes outlying the values used in our analyses. To maximize the clarity of the provided explanations, we also kept the further description of those parameters present in the Representative Results section.

8. Some of the highlighted steps cannot be filmed. These are abstract decision making steps such as Step 1.2 and calculations.

We thank the Editor for his comment. We have reviewed all the steps highlighted for being filmed in the previous manuscript version, and made sure to solely keep the ones that can indeed be filmed. This led to the removal of the abstract decision steps (Section 1.2). Calculations were not included in any step to record.

9. If step 2.3 is to be filmed, steps 2.1-2.2 should be as well.

We agree with the Editor that in the previous manuscript version, Sections 2.1 and 2.2 should have been selected for being filmed alongside Section 2.3. In the reworked content, those different steps have been merged together and are now collectively picked for being filmed.

10. Please obtain explicit copyright permission to reuse any figures from a previous publication. Explicit permission can be expressed in the form of a letter from the editor or a link to the editorial policy that allows re-prints. Please upload this

information as a .doc or .docx file to your Editorial Manager account. The Figure must be cited appropriately in the Figure Legend, i.e. "This figure has been modified from [citation]."

We thank the Editor for reminding us about the need to obtain explicit copyright permission to reuse previous publication figures. We verified that the content from our previous publication from which part of the present figure content is borrowed, can be reused without further permission steps, as per the Creative Commons Attribution License:

"*This article is available under the terms of the Creative Commons Attribution License (CC BY) (which may be updated from time to time) and permits use, distribution and reproduction in any medium, provided that the Contribution is properly cited.*"

Thus, we have simply stuck with citing the Figure in the appropriate legends.

Reviewer 1

Manuscript Summary:

This manuscript describes a useful analysis pipeline, which will likely become more used after this well-written tutorial

We thank the Reviewer for his positive comments about our manuscript.

Major Concerns:

Not sure if I can call this a concern, but if I think about a "video of an experiment" I am not sure that I would think about a tutorial on a pipeline. In particular I don't know to which extent a video describing this tutorial would be more explanatory than the tutorial itself. All of this hypotetically because I was not requested to review a video, but just the protocol, which I also find confusing, but that's not your fault.

We understand the point made by the Reviewer. When submitting the present manuscript, two parallel lines of thought strengthened our confidence about the relevance of a video tutorial:

1. Such approaches have been previously used, quite successfully, in publically available content about various neuroimaging software (see for example https://www.youtube.com/watch?v=6Xn6NC6ifUY for introductory material about how to correctly use SPM, or https://www.youtube.com/playlist?list=PLIQIswOrUH6_DWy5mJlSfj6AWY0y9iUce for a series of videos on how to use the Freesurfer software). We reasoned that a video-based support on how to deploy our computational pipeline might, similarly, ease the understanding of its different steps.

2. Our pipeline is particularly suited to a video format, since it enables to extract specific moments of a dynamic paradigm where there is a significant change in cross-subject brain synchronization. On top of the protocol details provided in written, and the guided tutorial on how to apply the pipeline, we also thought about incorporating some extracts of the analyzed movie in the video resource, alongside the associated triggered whole-brain connectivity changes. We will be working towards this goal during the recording stage of the publication process.

Also, in the experiment you describe also the ethics committee procedure, and the data acquisition. Of course these are fundamental steps for the experiments, but what you plan to describe in the video is the analysis right? Or will we see a video of you writing an ethical protocol application or potting people in the scan? It would be better to separate the preliminary steps as data acquisition (since the analysis can be run on data acquired by a third party and shared), and the analysis pipeline.

The Reviewer makes a very relevant remark, which was also raised by the

Editor. According to the JoVE article submission rules, all steps required towards the achievement of the analysis, including the ethics and acquisition steps, must be present within the written version of the protocol. However, only the steps that have been underlined in yellow within the text will be taken into consideration at the video recording stage.
In other words, we do not plan on being recorded while writing an ethical protocol application, hence why this particular protocol step is not part of the underlined material. Our thought is to display (1) a guided tutorial on how to apply our computational pipeline, and (2) actual results obtained from the analyzed movie (*i.e.*, movie extracts and associated elicited whole-brain changes).

Short TR: is it feasible to limit the scan to a certain brain region in order to minimize the TR? Also, is the protocol still valid for multiband acquisition?

We thank the Reviewer for his/her valuable question. It is indeed feasible to limit the scanning to a more localized brain region, either to minimize the TR of the experiment, or to focus on a given brain sub-structure with greater spatial accuracy. We have added this information as a protocol note in Section 2.A:

"*Note: The protocol can also be applied with a more restricted field of view (e.g., for analyses restricted to a specific brain sub-structure), which would enable either a better temporal resolution (lower TR), or a spatially more precise analysis.*"

Scrubbing: what happens if you scrub some time points from a subject and not from others? This issue could be better clarified.

We thank the Reviewer for raising a very relevant point: going back through the protocol details, we realized that we indeed did not provide sufficiently clear explanations about the scrubbing step.

As has now been added in Section 4.C.VII as a dedicated note, cubic spline interpolation was applied to the scrubbed data volumes in order to replace them with estimated values, using neighboring data points. Thus, we conserve a similar amount of data for all subjects. The added part reads:

"*Note: Cubic spline interpolation is performed on the scrubbed data points to replace them with estimated values from neighboring samples.*"

As specified in the Representative Results section (third paragraph), we selected a threshold of 10 % of scrubbed frames: above that value (a very conservative choice with regard to the fMRI literature), we discarded the whole session rather than including it in our analyses, because we judged that then, the interpolation process may not be sufficiently stable (for instance, if too many data points are scrubbed next to each other).

In our example results, we visually checked that preprocessed time courses following the scrubbing step did not contain any salient artifacts, which is enabled by the display of the second pipeline Graphical User Interface (see the

atlased time courses displayed in Supplementary Figure 2). We added a sentence to Section 4.C.IX to encourage the users to go through the same visual inspection process:

"*Verify, by visual inspection, that following the selected preprocessing steps, those output signals do not incorporate salient artifactual components.*"

Additionally, we remark that we also mention the motion correction issue in the Discussion (fourth paragraph): on top of suggesting possible additional cleaning tools for cases in which motion is particularly problematic (typically, some diseased populations), we now added a mention of the importance to also include motion parameters as covariates in any statistical analysis:

"[...] *we recommend that on top of including motion variables as covariates in the performed statistical analyses, additional preprocessing steps be run* [...]"

We hope that those changes and additions will be judged sufficient by the Reviewer to make the reader aware of the motion problematic in fMRI analysis.

Reviewer 2

Manuscript Summary:

The authors describe a method to analyze brain functional connectivity responses to naturalistic data, in this case a movie, in a time-varying fashion incorporating cross-subject synchronization of connectivity to specific events during the movie. The method seems sensible and is in general explained well in the manuscript.

We thank the Reviewer for his/her positive assessment of our work.

Major Concerns:

I found it difficult to understand how the bootstrapping procedure works and what role the rest acquisition(s) play in this. As far as I know, to assess whether meaningful (or true) non-stationarity of connectivity occurs is to test this against a null-distribution of windowed connectivity derived from e.g. phase-shifted time series. Why would one not do this here as well, and why would one need rest data to assess the validity of connectivity dynamics during a movie?

We thank the Reviewer for raising an issue that we find was indeed not properly discussed in the previous manuscript version. First, we want to emphasize that the bootstrapping procedure (which enables to lower the possible impact of outliers in the computations of ISFC), and the use of resting-state data as a null distribution (which enables, at a later analytical stage, to threshold the ISFC time courses and retain only statistically significant excursions), are two separate computational aspects. We answer the latter concern here, and come back to the bootstrapping aspect in a later answer to the Reviewer's comments.

The Reviewer is right that a typical way to test for the presence of non-stationarity in fMRI data is to generate null time courses through phase randomization procedures, and compare the actual data to those surrogates.

In principle, nothing prevents the application of that approach to the movie time courses studied here: an obvious advantage would then be the lower scanning duration, since purely resting-state sessions would then not be required anymore.

However, in our work, we opted for the resting-state approach given that (1) we had this data to our disposal, so why not use it, and (2) we judged it a cleaner approach to the generation of surrogate data.

Regarding this second point, we reasoned that in phase-randomized data, although second-order information is kept, higher-order features from the data are not. Perhaps those actually are important to the proper characterization of fMRI data, and still lie in purely intrinsic (not movie-driven) functional activity as well. The efficacy of analytical approaches such as Independent Component Analysis lends further support to that hypothesis.

In order to more thoroughly investigate the difference between the resting-state and the phase-randomization null generation approaches, we applied both to a subset of our data (the 12 combined movie/resting-state sessions shared within the scope of this work) with similar analytical parameters (framewise displacement threshold of 0.5 mm, window size W = 10 TR, step size 1 TR, 250 bootstrapping folds, 6 session segments in the reference group, α-level = 0.05 %), and compared the connections that were extracted as showing significant ISFC changes across the two cases. The results are presented in the newly added Supplementary Figure 5: when representing the percentage of time points detected as showing a significant excursion, the same overall pattern across connections can be observed when the phase-randomized (red plots) or resting-state (blue plots) data are used for null generation. However, the percentage of detected time points showing a significant ISFC change is consistently larger in the phase-randomization case, which demonstrates that in accordance with our expectations, this particular null hypothesis is not as strong, and may be prone to a larger detection of false positives.

We have appended a brief mention of those results in our Discussion (second paragraph), when referring to the importance of properly tailored significance assessment methods in dynamic functional connectivity approaches, and added Supplementary Figure 5 to our submitted material:

"As an alternative approach to avoid the additional resting-state recordings, we also offer the possibility to generate phase-randomized data directly from the stimulus-related time courses, an approach often used in dynamic functional connectivity analyses[23,24]. Further evaluation on a subset of sessions revealed that although the resting-state null method is more conservative, and thus less prone to false positives, the global patterns of ISFC excursion detection were similar across both schemes (see Supplementary Figure 5).

[Place Supplementary Figure 5 here]"

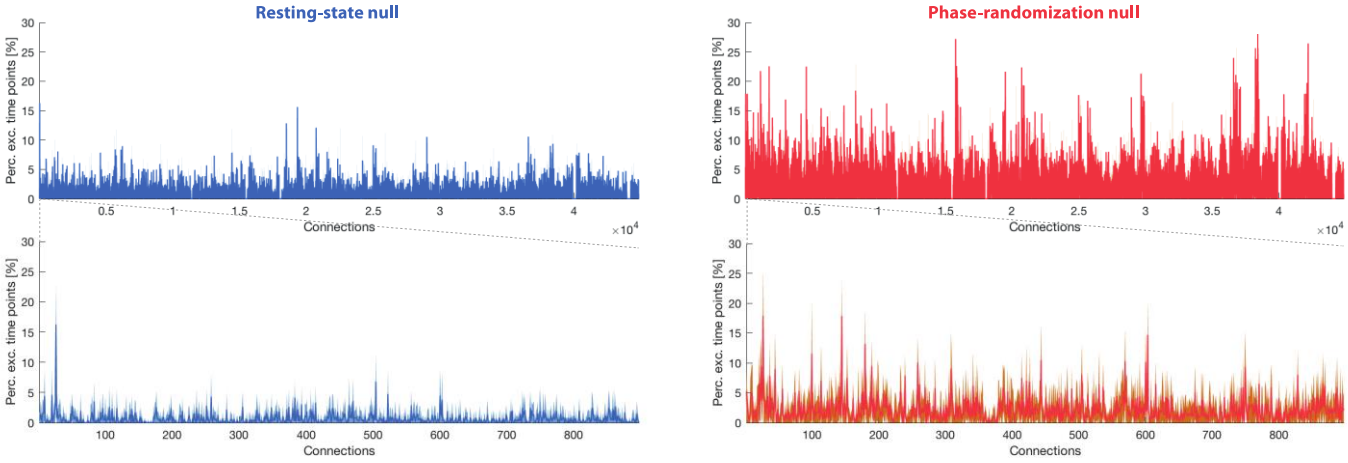

Supplementary Figure 5: Detection of ISFC excursions across null data generation methods. For resting-state (left column, blue plots) or phase-randomization (right column, red plots) null data generation methods, percentage of ISFC excursions extracted across connections. The bottom plots are an inset on the connections emanating from the first three considered brain regions. Error represents standard deviation across subjects.

Since we understand that recording time may sometimes be more valuable than the gain in accuracy of the exact used null data generation scheme, we have also implemented the alternative phase-randomization strategy into our pipeline, and mentioned in Section 2.B of the protocol that it may be an alternative to the recording of resting-state data:

"Note: If it is not desired to go through the aforementioned additional resting-state acquisition, an alternative (albeit more prone to the detection of false positives; see Discussion) computational option in the pipeline replaces this data by surrogate time courses computed from the paradigm-related signals (see step 5.A.II)."

Specifically, rest data do not necessarily constitute "appropriate null data". As the authors mention, there could be spillover effects of previous tasks on the rest period. The authors provide a further note at 2.4 that "Separate stimulus-related and resting-state acquisitions prevent otherwise possible interplays between the conditions". It is therefore surprising that both the rest scan directly following the movie and the separate rest scan were not made before the movie paradigm instead.

The Reviewer is absolutely right that resting-state data acquired shortly after the movie paradigm do not necessarily constitute appropriate null data given possible spillover effects, as we ourselves already mention in Section 2.B of the protocol.

In our analyses, we included both those possibly "corrupted" resting-state, and purely resting-state recordings, to the set of considered data, because our amount of available null data would otherwise not have enabled us to threshold movie-watching time courses at a sufficiently stringent statistical level. Actually, an α-value of 0.01 % as used in our presented results is already quite less stringent than what would be required according to Bonferroni correction, and could be achieved thanks to the combined pool of resting-state data; we get back in more details to the mathematical side of the thresholding process in answering a later question from the Reviewer (see Minor Concerns).

We reasoned that if anything, possible spillover effects, on top of being partly "diluted" by the parallel presence of purely resting-state recordings, would prevent the detection of some movie-responsive connections, rather than driving the erroneous detection of false positives.

We have now added, in the Representative Results section (second paragraph), a specification that separate resting-state acquisitions were strongly encouraged, and that our actual choice of mixing the use of post-movie and purely resting-state data for null distribution generation was due to the requirement for a larger amount of data points:

"Importantly, our acquisition protocol was not optimal in the sense that resting-state recordings acquired just after movie exposure may be partly corrupted by spillover effects; we make use of this data in the present findings to have a

satisfying amount of samples for statistical thresholding, but this should be avoided whenever possible."

Did I understand correctly that the different rest data (i.e., twice directly after the movie, and once after the two movie/rest runs) were aggregated? How is this done exactly, and why would this be the best reference material and not just the rest scan after the two movie runs?

Yes, the Reviewer correctly understood that all available resting-state data were aggregated together. As explained above, the main reason for this aggregation as compared to solely resorting to "pure resting-state" data is the otherwise too low amount of data points in the null distribution for thresholding (see Minor Concerns below for more details on the mathematical explanation).

Under 5.1.4, what is meant with "session"? Does this refer to the movie and rest (parts of the) scans?

A session refers to either a combined movie/rest scan (referred to as RUN_1 or RUN_2 in Figure 1), or a purely rest scan (referred to as RUN_3). We have clarified this point in a dedicated protocol note (Section 5.A.IV):

"Note: A session in the present work may refer either to a combined movie/resting-state recording (termed RUN_1 and RUN_2 in Figure 1A), or to a purely resting-state recording (RUN_3). A session segment refers to a sub-portion of a session recording, either when the movie was watched, or when the subjects lied at rest."

In addition, we modified Section 5 to avoid a misuse of the "session" terminology: throughout several protocol sub-points, the user is required to work with a specific segment of a recording session (for example, only the time interval when the movie was being watched). This has also been explicitly clarified in the above note, and whenever referring to those sub-portions of a session, we now use the "session segment" terminology.

And under 5.A.VII, does "reference group" refer to the rest periods from all subjects, and session subtypes to the different types of rest acquisitions?

In Section 5.A.VII, "reference group" refers to a subset of session segments that act as the point of comparison to which data from session segment s is compared. For example, if considering the movie-watching session segments (by appropriately selecting this temporal interval in Section 5.A.VI), the data for session segment s (the s^{th} movie-watching recording) will be compared to a set of other session segments randomly selected from the dataset (that is, to the movie-driven functional activations from other subjects).
This process will be repeated many times, each time sampling a different reference group for the computations. This step ensures further robustness of the ISFC estimates, to account for the possible presence of outlier data points.

We now give those details in a dedicated protocol note (Section 5.A.VII):

"Note: The reference group is the set of session segments to which the functional time courses of session segment s are compared at each fold of the bootstrapping process. For the results to be more robust to outlier data points, ISFC is computed multiple times on a different reference group (that is, a different subset of session segments)."

We also remark that in Section 5.A, we specifically mention that the following protocol sub-points should be run separately for each session segment subtype; we reckon that the former misuse of "session", instead of "session segment", in those explanations, may have confused the reader, and corrected this unfortunate inaccuracy.

These issues need to be addressed in more detail to be able to better understand the statistical procedures.

We hope that the adjustments mentioned above enable a better understanding of the statistical procedures introduced in the manuscript. We remain open to modify any remaining issue that the Reviewer may still have.

Minor Concerns:

- "resting-state and task-evoked activity patterns are increasingly understood to embed important specificities". This is a bit vague.

We have modified the previous formulation into a clearer variant:

"This is important because resting-state and task-evoked activity patterns are increasingly understood to be characterized by distinct properties[21,22]."

- Hierarchical numbering should be done less ambiguously, especially these are also referenced as such, e.g.: 3/3.1/3.1.1.

We thank the Reviewer for his/her valuable suggestion. We have now modified the numbering so that different sets of symbols highlight specific hierarchical levels: the first level is now denoted by (1,2,3...), the second level by (A,B,C...) and the third level by (I,II,III...).

- 4.2.5: "probabilistic tissue map" - would add that these are individually derived maps, not a template.

In fact, the maps are templates originating from the DPARSFA toolbox, whereas the averaged signals are of course themselves session-specific. This has been clarified in the newer manuscript version (Section 4.B.V):

"Note: The regression step is inspired from a function originating from the DPARSFA toolbox[29]. The white matter and cerebrospinal fluid signals from individual subjects are averaged over the voxels for which the respective template DPARSFA probabilistic tissue map showed a signal larger than 0.99."

- "Time points at which a stimulus-related ISFC value statistically significantly exceeds the null distribution are tagged as -1/+1 for significant ISFC decreases and increases, respectively." - In the plots the peaks never reach -/+1. Are these then not significant? Probably I am misunderstanding the thresholding.

The Reviewer did not misunderstand the thresholding process, which indeed tags data points with +1 or -1 when, respectively, a significant ISFC increase or decrease is established. The apparent mismatch with the plots from Figure 2A and Supplementary Figure 4 comes from the fact that we displayed averaged ISFC excursion time courses across subjects: a value of 1 would then imply that all subjects showed a similar ISFC increase/decrease at the same time point (*i.e.*, that all were tagged as +1/-1). For this reason, we have been using "Subject fraction" as the y-axis label in those plots.

To render this point clearer, we have now modified the legend of Figure 2:

"*ISFC transient time courses, averaged across subjects, for three indicative connections* [...]"

Note that the cross-subject average use is also what enables to display, on top of the mean excursion time course, an associated confidence interval.

- "As an indication, for n = 299 atlas regions as here and given our tally of 5762 resting-state data points, we could at best achieve an α-value close to 0.01 %." - This should be described in the methods and in a bit more detail. I don't understand the math here.

We understand the difficulties from the Reviewer; the alluded point is actually also important to properly answer some of the above comments.

As stated in the manuscript, we had a total amount of 5'762 data points left following sliding-window ISFC computations on our resting-state data.

For 299 atlas regions, there is a total of 299*298/2=44'551 connections to consider. If a statistical level of α=0.05 is desired (that is, a false positive rate of 5 %), since parallel statistical testing is performed for each connection and considering marginalization across subjects, one should actually resort to the corrected α-value $0.05/44'551 = 1.12 \cdot 10^{-6}$.

To achieve a one-sided α-level of 0.05, one would need to use the maximal value of a null distribution made of 19 samples as the significance threshold. Indeed, a more extreme actual value would then exceed 95 % of available measures (19 out of 20, or all except itself), hence the desired 5 % level.

To achieve a two-sided α-level of 0.05 as defined in our manuscript (see Section 5.B.VII), one would require the equivalent number of samples as for a one-sided α-level of 0.1, that is, 9 null samples.

By applying a similar reasoning with 5'762 data points, we can at best reach a significance level of $8.68 \cdot 10^{-5}$, which is not quite as stringent as what would be required according to Bonferroni correction. We rounded this to $\alpha=10^{-4}$ in our work.

We have added those explanations in the newer manuscript version to clarify this statistical thresholding step (see Section 5.B.VI):

"*Note: In our analyses, we had 5'762 resting-state data points to our disposal, and selected an α-value of 10^{-4}. This means that we wanted 0.01 % of data samples to be larger or equal to the selected thresholds past which an ISFC excursion would be deemed significant. For comparison purposes, the α-level demanded by Bonferroni correction would be $0.05/44'551=1.12 \cdot 10^{-6}$, and the most stringent possible α-level enabled with our amount of data (n samples) would be $\frac{1}{2n+2} = 8.68 \cdot 10^{-5}$.*"

Further, we remark that given the dependence of the different connections (299 separate connections share the same brain region at one of their end, and even distinct but structurally strongly linked areas may also be expected to share some functional similarity), the "true" statistical level at which the data should be thresholded to avoid the presence of false positives lies somewhere between 0.05 and $1.12 \cdot 10^{-6}$.

We empirically found that using the most conservative possible level with our amount of data, the key ISFC patterns standing out in the analyses could easily be interpreted with respect to the associated movie cues, lending support to the hypothesis that we already manage to discard a large fraction of the possible false positive detections. This is further confirmed by the time-locked nature of extracted ISFC transients across subjects.

- What would be a critical amount of bad movement volumes (FD > 0.5) to consider the participant's data unfit for further analysis? Given the rather small number of TRs used as windows (5 or 10), correlations in these windows should be quite unstable already, and would easily be strongly confounded by scrubbing. The authors should comment more on these issues.

The Reviewer raises an important point, which is the proper handling of motion in the analyzed data. In fact, we already set a criterion for discarding a participant's data in the previous manuscript version; indeed, as written in the Representative Results part (paragraph 3):

"*We excluded all sessions for which more than 10 % of frames were scrubbed, at a threshold of 0.5 mm* [...]"

Below 10 % of corrupted frames, the data was kept and cubic spline interpolation was used to replace the scrubbed data points using the information from neighboring samples (as now explicitly mentioned in Section 4.C.VII). Above 10 %, we simply discarded the data and did not include it in the analyses.

This value of 10 %, compared to typical dynamic functional connectivity analysis standards (see *e.g.* references 25 or 31), is quite a conservative choice, in part because we rely on a low number of samples in our sliding-window estimates. A few other remarks are worth a mention:

1. The use of an inter-subject framework may actually further mitigate the influence of motion compared to the more traditional "within-subject" sliding-window functional connectivity computations, since the deleterious impacts of motion on the signals from different subjects may not occur at the same moments in time.

2. Although we indeed use a small number of values for our estimates, we resort to the same number of samples when computing sliding-window ISFC measurements on our null data, and so, the possible confounding influence of motion is also present in the null distribution used at the thresholding stage. This step can thus, to an extent, be seen as providing an "extra protection" against motion-related artifacts.

3. Given the importance of the motion question, we also devote a paragraph from our Discussion (paragraph 4) to this question; there, we highlight both the need to include motion parameters as covariates in any statistical comparison process (an addition to this newer manuscript version), and also some additional, optional motion correction strategies that can be used on top of the introduced pipeline.

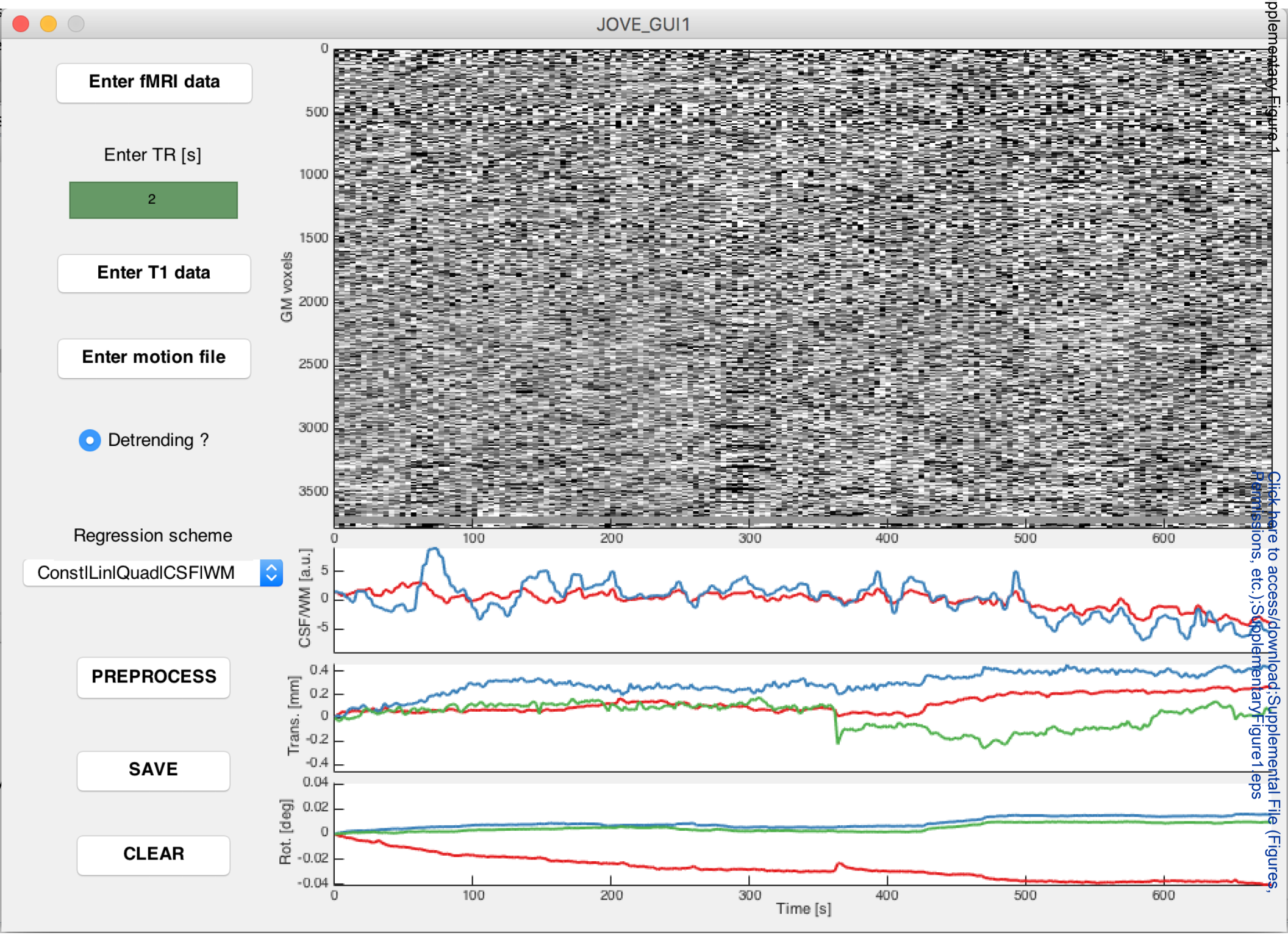

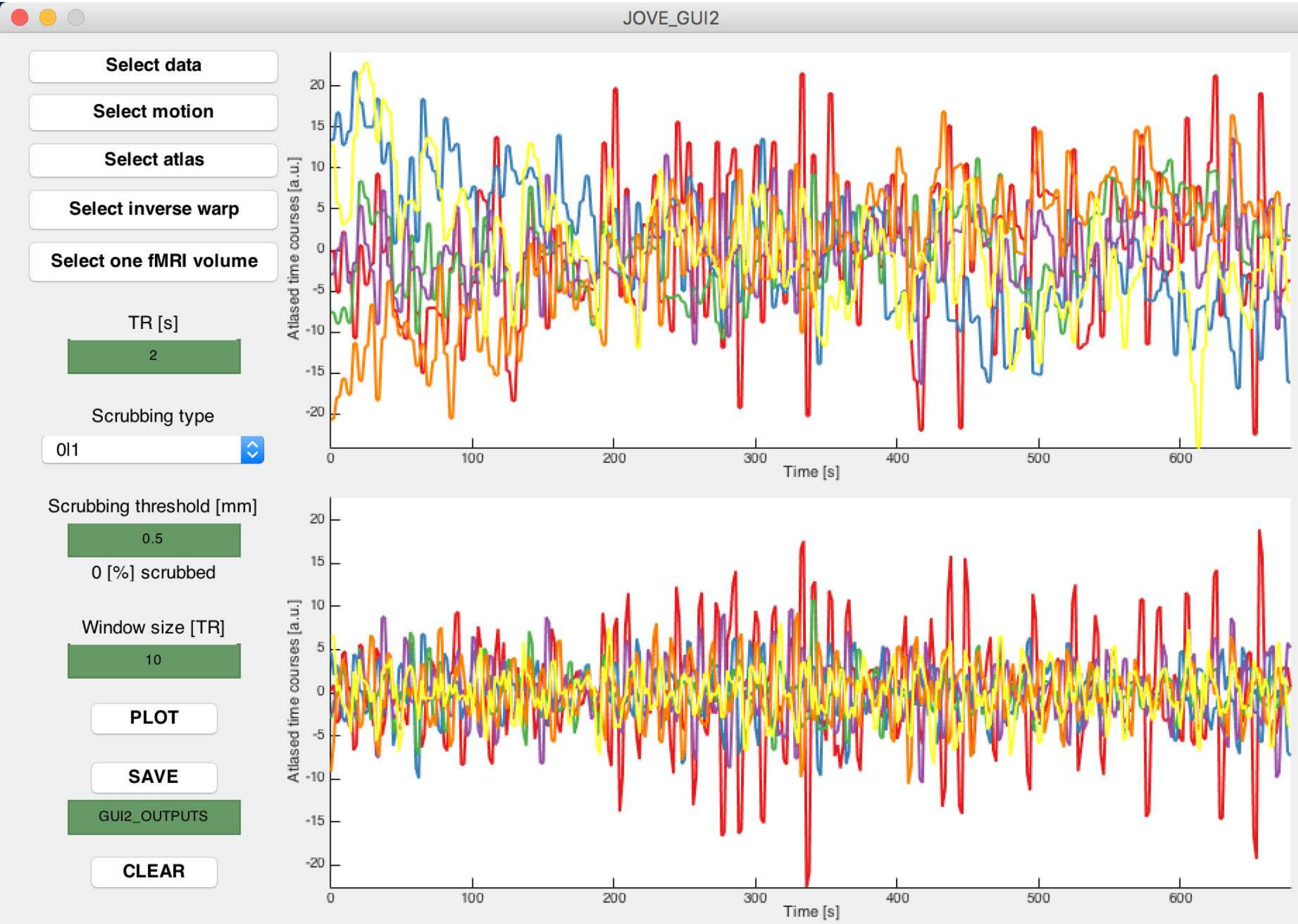

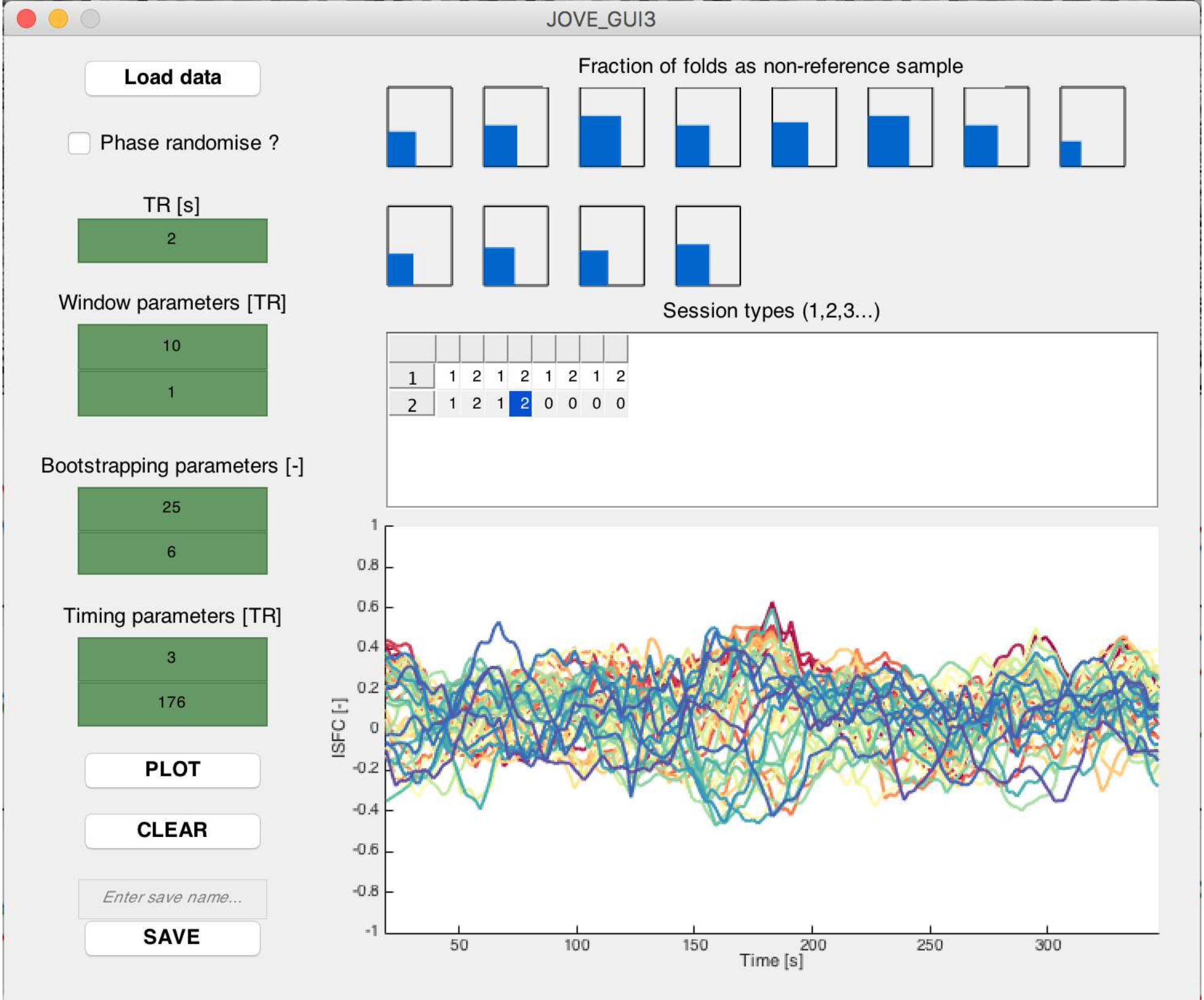

Supplementary Figure 4

Click here to access/download;Supplemental File (Figures, Permissions, etc.);SupplementaryFigure4.eps

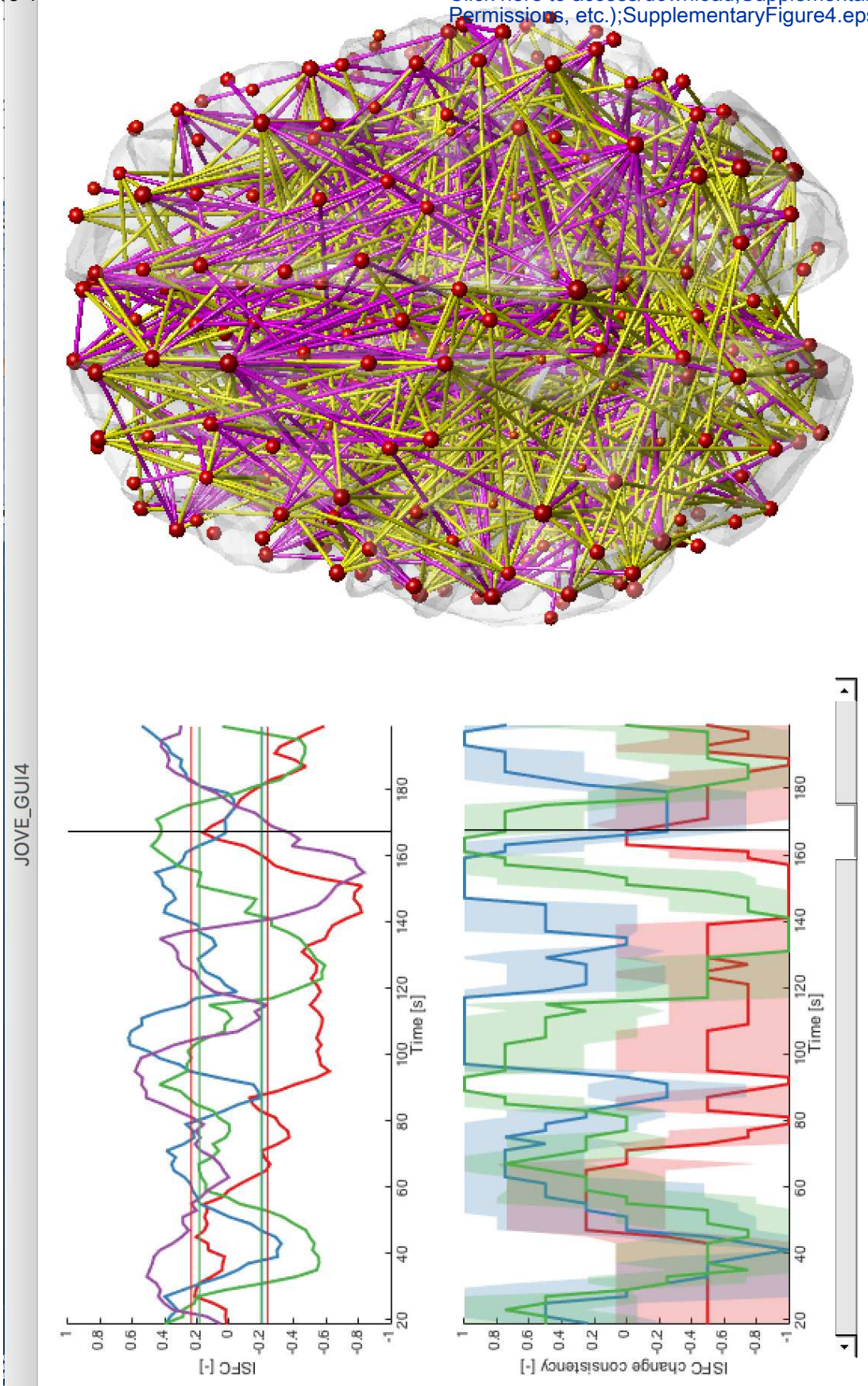

Supplementary Figure 5

Click here to access/download;Supplemental File (Figures, Permissions, etc.);SF5.eps